Molecular Therapy
Original Article

Function of Novel Anti-CD19 Chimeric Antigen Receptors with Human Variable Regions Is Affected by Hinge and Transmembrane Domains

Leah Alabanza,[1] Melissa Pegues,[1,3] Claudia Geldres,[1,3] Victoria Shi,[1] Jed J.W. Wiltzius,[2] Stuart A. Sievers,[2] Shicheng Yang,[1] and James N. Kochenderfer[1]

[1]Experimental Transplantation and Immunology Branch, National Cancer Institute, Bethesda, MD 20892, USA; [2]Kite Pharma, Inc., Santa Monica, CA 90404, USA

Anti-CD19 chimeric antigen receptor (CAR) T cells have caused remissions of B cell malignancies, but problems including cytokine-mediated toxicity and short persistence of CAR T cells in vivo might limit the effectiveness of anti-CD19 CAR T cells. Anti-CD19 CARs that have been tested clinically had single-chain variable fragments (scFvs) derived from murine antibodies. We have designed and constructed novel anti-CD19 CARs containing a scFv with fully human variable regions. T cells expressing these CARs specifically recognized $CD19^+$ target cells and carried out functions including degranulation, cytokine release, and proliferation. We compared CARs with CD28 costimulatory moieties along with hinge and transmembrane domains from either the human CD28 molecule or the human CD8α molecule. Compared with T cells expressing CARs with CD28 hinge and transmembrane domains, T cells expressing CARs with CD8α hinge and transmembrane domains produced lower levels of cytokines and exhibited lower levels of activation-induced cell death (AICD). Importantly, CARs with hinge and transmembrane regions from either CD8α or CD28 had similar abilities to eliminate established tumors in mice. In anti-CD19 CARs with CD28 costimulatory moieties, lower levels of inflammatory cytokine production and AICD are potential clinical advantages of CD8α hinge and transmembrane domains over CD28 hinge and transmembrane domains.

INTRODUCTION

Chimeric antigen receptors (CARs) are fusion proteins incorporating an antigen recognition moiety and T cell signaling domains.[1–6] In recent clinical trials, infusions of anti-CD19 CAR T cells have caused prolonged complete remissions of advanced B cell malignancies in many patients;[7–12] however, anti-CD19 CAR T cell therapies are still in an early stage of development, and many aspects of CAR T cell therapies are in need of improvement.[9–11,13] Anti-CD19 CAR T cells have been associated with toxicities including hypotension and a variety of neurological abnormalities.[7,9,10,12,14–16] Toxicities after infusions of anti-CD19 CAR T cells have been consistently associated with elevated serum levels of inflammatory cytokines.[7,9,10,12,14–16] Not all patients receiving anti-CD19 CAR T cells achieve lasting remissions of their malignancies, so improvement in anti-malignancy effectiveness is needed.[10,13,14,17,18] Anti-malignancy responses after CAR T cell infusions have been consistently associated with high levels of blood CAR T cells,[14,15,17,19,20] so an important general goal of CAR research is to develop approaches that increase the levels of CAR T cells in patients.

The antigen recognition domain of CARs is most commonly a single-chain variable fragment (scFv). All anti-CD19 CARs that have been tested clinically to date contain scFvs derived from murine monoclonal antibodies.[7,10–12,19,21] Anti-CAR immune responses targeting murine scFvs could eliminate CAR-expressing T cells and abrogate therapeutic effectiveness. T cell immune responses directed against anti-CD19 CAR transgene components have been reported.[11,14,17,22,23] Immune responses against CAR T cells might be especially problematic if repeated infusions of CAR T cells are administered to a patient. In the case of anti-CD19 CARs, T cell anti-CAR immune responses are probably a more important problem than humoral immune responses, because anti-CD19 CAR T cells eradicate normal B cells, which should prevent humoral anti-CAR immune responses.[8–10,15] With a goal of limiting anti-CAR immune responses, we have constructed novel anti-CD19 CARs containing variable regions from a fully human antibody. One anti-CD19 CAR with variable regions from a fully human antibody has been previously reported.[24]

CAR design has potential to affect the function of CAR-expressing T cells.[1,2,6,25,26] Selection of the hinge and transmembrane regions of the CAR fusion protein is a CAR design aspect that has been studied less than other aspects of CAR design. The hinge region of a CAR connects the scFv to the transmembrane portion.[6,27] The hinge and transmembrane regions of a CAR can potentially be important to the function of T cells expressing the CAR.[27–30] Activation-induced

Received 1 December 2016; accepted 25 July 2017;
http://dx.doi.org/10.1016/j.ymthe.2017.07.013.

[3]These authors contributed equally to this work.

Correspondence: James N. Kochenderfer, Experimental Transplantation and Immunology Branch, National Cancer Institute, 10 Center Drive, CRC Room 3-3330, Bethesda, MD 20892, USA.
E-mail: kochendj@mail.nih.gov

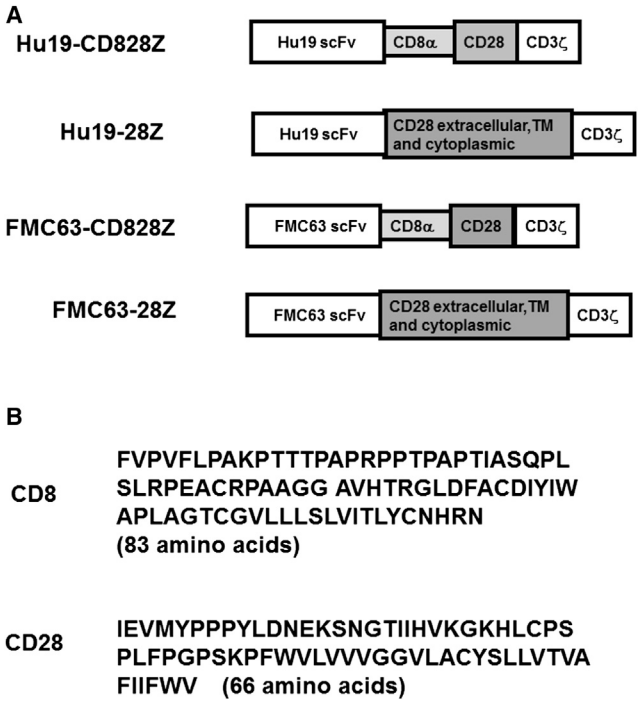

Figure 1. Anti-CD19 CARs with Either Human or Murine scFvs Were Constructed

(A) Schematics of all CARs studied are shown. Two anti-CD19 CARs incorporating fully human human variable regions were constructed and designated Hu19-CD828Z and Hu19-28Z. Hu19-CD828Z contained the Hu19 scFv, the extracellular hinge region of the human CD8α molecule, the transmembrane (TM) region of CD8α, the entire intracellular region of human CD28, and the CD3ζ T cell activation domain. Hu19-28Z included the Hu19 scFv, the extracellular hinge portion of human CD28, the transmembrane region of CD28, the entire intracellular region of CD28, and the CD3ζ T cell activation domain. The FMC63-CD828Z CAR had the same structure as Hu19-CD828Z except for substitution of the murine FMC63 scFv for the human Hu19 scFv. The FMC63-28Z CAR had the same structure as Hu19-28Z except for substitution of the murine FMC63 scFv for the human Hu19 scFv. (B) The amino acid sequence of the human CD8α extracellular and transmembrane regions had 83 amino acids. The amino acid sequence of the human CD28 extracellular and transmembrane regions included 66 amino acids.

cell death (AICD) is a process by which T cell activation leads to apoptosis of T cells.[28–32] To investigate how CAR hinge and transmembrane components affect the biology of anti-CD19 CAR T cells, we have conducted experiments with CARs containing hinge and transmembrane regions from either the human CD28 molecule or the human CD8α molecule. We found that these different hinge and transmembrane regions have an impact on CAR T cell cytokine production and susceptibility to AICD.

RESULTS

Design of Novel Anti-CD19 CARs with Fully Human Variable Regions

We set out to develop a new anti-CD19 CAR with a fully human amino acid sequence except for the linker peptide in the scFv and the junctions between each component of the CAR sequence, such as the junction between the CD28 and the CD3ζ components. To assess two hinge and transmembrane regions, we used a series of four CARs (Figures 1A and 1B). Hu19-CD828Z incorporated the Hu19 scFv, hinge and transmembrane regions from the human CD8α molecule, a CD28 costimulatory domain, and a CD3ζ T cell activation domain. Hu19-28Z had the same sequence as Hu19-CD828Z except that Hu19-28Z had hinge and transmembrane regions from human CD28 instead of CD8α. FMC63-CD828Z and FMC63-28Z had the murine FMC63 scFv in place of the human Hu19 scFv.

CARs with the Hu19 scFv Specifically Recognize CD19, and They Recognize Target Cells in a Similar Manner to CARs with FMC63-Derived scFvs

Exquisite antigen-specificity is a prerequisite for any CAR to be used clinically. To assess the specificity of the Hu19 scFv, we cultured Hu19-CD828Z-expressing T cells with a variety of target cells overnight. We performed a standard ELISA on the culture supernatant to detect interferon (IFN)-γ release as a marker of target cell recognition by the T cells. We found that T cells expressing Hu19-CD828Z specifically recognized $CD19^+$ target cells and exhibited minimal IFN-γ release in response to CD19-negative target cells (Table 1). We also compared Hu19-CD828Z-expressing T cells with FMC63-CD828Z-expressing T cells for recognition of $CD19^+$ and CD19-negative target cells. We found that both CARs specifically recognized the $CD19^+$ target cells. The amount of IFN-γ produced by Hu19-CD828Z-expressing T cells in response to $CD19^+$ target cells was generally higher than the amount of IFN-γ produced by FMC63-CD828Z-expressing T cells from the same donor (Table 2). We did not find a difference in the ability of FMC63-CD828Z versus Hu19-CD828Z to kill target cells in vitro (Figure S1) or eradicate tumors in mice (Figure S2).

Functional Assessment of Fully Human Anti-CD19 CARs with Different Hinge and Transmembrane Regions

We hypothesized that incorporation of different hinge and transmembrane domains might affect the function of Hu19 CARs. As an initial step in evaluating the function of T cells expressing CARs with these different hinge and transmembrane regions, we conducted a series of experiments in which human T cells expressing either Hu19-CD828Z or Hu19-28Z were evaluated for degranulation and cytokine release. We found that Hu19-CD828Z and Hu19-28Z were expressed on the surface of transduced T cells at similar levels when assessed by flow cytometry (Figure 2A). Nonetheless, degranulation and ELISA results were normalized for CAR expression in all experiments. We assessed degranulation by measuring the difference in cell-surface CD107a expression when CAR-expressing T cells were stimulated with either the $CD19^+$ target cell NALM6 or the CD19-negative target cell NGFR-K562 (Figure 2B). Compared with $CD8^+$ T cells expressing Hu19-CD828Z, a modestly higher percentage of $CD8^+$ T cells expressing Hu19-28Z specifically degranulated in response to $CD19^+$ NALM6 cells (Figure 2C). In contrast, there was not a statistically significant difference in degranulation when $CD4^+$ T cells expressing either Hu19-CD828Z or Hu19-28Z were stimulated

Table 1. Specificity of Hu19-CD828Z

Effector T Cells	CD19-K562	Primary CLL	A549	MDA-MB231	293T	TC71	CCRF-CEM	T Cells Alone[a]
Hu19-CD828Z	29,198	3,922	<12	<12	26	26	171	101
Untransduced	431	123	<12	<12	143	28	21	<12

T cells transduced with LSIN-Hu19-CD828Z or left untransduced were cultured with the indicated target cells overnight, and a standard IFN-γ ELISA was performed. All values are in picograms per milliliter of IFN-γ. The CD19-K562 and primary CLL cells are $CD19^+$ target cells. A549, MDA-MB231, 293T, TC71, and CCRF-CEM are CD19-negative target cells. Similar results were obtained in five experiments with cells from five different donors.
[a]CAR T cells cultured without any target cells.

with NALM6 target cells (Figure 2D). For both $CD8^+$ and $CD4^+$ T cells, no statistically significant difference in degranulation between Hu19-CD828Z and Hu19-28Z was observed when $CD19^+$ primary human chronic lymphocytic leukemia (CLL) cells were used as $CD19^+$ target cells (Figures 2E and 2F). Inflammatory cytokines are an important cause of toxicity after CAR T cell infusions in humans,[9,14–16,33] so it is important to assess inflammatory cytokine production by new CARs. We compared release of IFN-γ and tumor necrosis factor (TNF)-α by T cells expressing either Hu19-CD828Z or Hu19-28Z after the T cells were cultured overnight with NALM6 cells. IFN-γ and TNF-α release was significantly less with T cells expressing Hu19-CD828Z versus T cells expressing Hu19-28Z (Figures 2G and 2H). The raw cytokine values for the data shown in Figures 2G and 2H are in Tables S1 and S2, respectively.

Next, we attempted to generalize the functional differences between CARs with hinge and transmembrane regions derived from either CD8α or CD28 by assessing CARs containing the murine FMC63 scFv. We compared the FMC63-CD828Z CAR with hinge and transmembrane regions from CD8α to the FMC63-28Z CAR with hinge and transmembrane regions from CD28. FMC63-CD828Z and FMC63-28Z were expressed at similar levels on the surface of transduced T cells (Figure 3A). Similar to our results with Hu19-containing CARs, a modestly higher percentage of degranulation was observed with $CD8^+$ T cells expressing FMC63-28Z than with $CD8^+$ T cells expressing FMC63-CD828Z (Figures 3B and 3C). No difference was observed in the level of degranulation of $CD4^+$ T cells expressing FMC63-CD828Z versus FMC63-28Z (Figure 3D). As with CARs containing the Hu19 scFv, we found that IFN-γ and TNF-α release was significantly less with T cells expressing FMC63-CD828Z versus T cells expressing FMC63-28Z (Figures 3E and 3F). The raw cytokine values for the data shown in Figures 3E and 3F are in Tables S3 and S4, respectively.

Despite Different Levels of Cytokine Release, T Cells Expressing Hu19-CD828Z and Hu19-28Z Exhibited Similar Levels of Proliferation

In accordance with the similar levels of CD19-specific degranulation with Hu19-CD828Z and Hu19-28Z (Figures 2 and 3), we did not find a consistent difference in the ability of Hu19-CD828Z and Hu19-28Z to kill $CD19^+$ target cells in vitro (Figures 4A and 4B). We did not find a consistent difference in CD19-specific proliferation as measured by carboxyfluorescein succinimidyl ester (CFSE) dilution when T cells expressing the two CARs were compared (Figure 4C). Consistent with the CFSE dilution result, we also did not find a consistent difference in the CD19-specific increase in CAR^+ T cell numbers when the two CARs were compared during the 4-day CFSE dilution assays (Figure 4D), although there was a trend that was not statistically significant ($p = 0.12$) toward a larger increase in T cell number with T cells expressing Hu19-CD828Z. We assessed T cells expressing either Hu19-CD828Z or Hu19-28Z for CD19-specific interleukin (IL)-2 release. Similar to the results with IFN-γ and TNF-α, the amount of IL-2 released was less among T cells expressing Hu19-CD828Z than among T cells expressing Hu19-28Z (Figure 4E). The raw IL-2 values for the data shown in Figure 4E are in Table S5.

Levels of CD19-Specific CD3ζ Phosphorylation Were Lower with Hu19-CD828Z Than with Hu19-28Z

Activation of T cells expressing CARs with CD3ζ domains involves phosphorylation of tyrosines in immune receptor tyrosine-based activation motifs (ITAMs) in the CD3ζ molecule.[34] As an assessment of CAR T cell activation, we measured the phosphorylation status of CD3ζ ITAM domains of Hu19-CD828Z and Hu19-28Z by intracellular flow cytometry. The results are expressed as CD3ζ phosphorylation after in vitro activation with $CD19^+$ target cells relative to CD3ζ phosphorylation after in vitro activation with CD19-negative target cells (Figure 4F). The level of CD19-specific CD3ζ phosphorylation was less with the Hu19-CD828Z CAR than with the Hu19-28Z CAR, which suggests that a weaker T cell activation signal is transmitted by Hu19-CD828Z compared with Hu19-28Z (Figure 4G). Raw data for the CD3ζ phosphorylation experiments is in Table S6.

Compared with Hu19-28Z-Expressing T Cells, Hu19-CD828Z-Expressing T Cells Underwent Less Antigen-Specific Activation-Induced Cell Death

To assess AICD in CAR-expressing T cells, we cultured T cells with either $CD19^+$ NALM6 cells or CD19-negative NGFR-K562 cells and assayed for apoptosis by staining the T cells with annexin V (Figure 5A). We found that T cells expressing either Hu19-CD828Z or Hu19-28Z cultured with $CD19^+$ target cells underwent substantial AICD in all 4 donors tested. The level of AICD was less among T cells expressing Hu19-CD828Z than among T cells expressing Hu19-28Z (Figure 5B). The AICD was dependent on cell-surface CAR expression and exposure to CD19 (Figure 5A).

To investigate the mechanism of the AICD in the CAR T cells, we stimulated CAR T cells in vitro with $CD19^+$ target cells or CD19-negative target cells and assessed active caspase-3 expression. We

Table 2. Comparison of Hu19 scFv and FMC63 scFv

	CD19-K562	NALM-6	Primary CLL	CCRF-CEM	T Cells Alone[a]
Patient 1					
Hu19-CD828Z	99,326	11,199	4,662	51	57
FMC63-CD828Z	58,463	3,895	2,291	61	62
Patient 2					
Hu19-CD828Z	92,058	20,864	29,698	67	73
FMC63-CD28Z	87,968	8,034	15,995	45	59

T cells from the indicated patients expressing the indicated CARs were cultured with the indicated target cells overnight, and a standard IFN-γ ELISA was performed. All values are in picograms per milliliter of IFN-γ. All values are normalized for differences in the fraction of T cells expressing the different CARs for each patient. The CD19-K562, NALM6, and primary CLL cells are all $CD19^+$ target cells. CCRF-CEM is a CD19-negative target cell.

[a]CAR T cells cultured without any target cells.

found that active caspase-3 expression was consistently higher in CAR T cells after stimulation with $CD19^+$ target cells versus CD19-negative target cells (Figures 5C and 5D). We did not see a difference in AICD when CARs containing Hu19 or FMC63 scFvs were compared (Figure S3).

Compared with T Cells Expressing Hu19-28Z, T Cells Expressing Hu19-CD828Z Underwent Less Activation-Induced Cell Death after Repetitive In Vitro CD19 Stimulation

T cells were stimulated with anti-CD3 on day 0 of culture and transduced to express either Hu19-CD828Z or Hu19-28Z on day 1 of culture. We assessed the expression of multiple surface markers 7 days after culture initiation; the only consistent differences were in central memory T cells and CD25, which were both higher with Hu19-CD828Z versus Hu19-28Z (Figures S4 and S5). On day 7 and again on day 10, the T cells were stimulated with CD19 by culturing with CD19-K562 cells. On day 12 of culture, T cell phenotype was assessed by flow cytometry. There was not any statistically significant difference between T cells expressing either Hu19-CD828Z or Hu19-28Z for the following markers: CD62L, T cell immunoglobulin and mucin-domain containing-3 (Tim-3), CD57, and CD25 (not shown). There was also not a statistically significant difference between T cells expressing Hu19-CD828Z and Hu19-28Z in the percentage of naive, effector memory, or central memory T cells as defined by CD45RA and CCR7 markers (not shown).[35] There was a borderline difference in CD69 expression ($p = 0.051$; Figure 6A). Compared with Hu19-CD828Z-expressing T cells, Hu19-28Z T cells expressed higher levels of both programmed cell death protein-1 (PD-1) and lymphocyte-activation gene-3 (LAG-3) (Figures 6B and 6C). High and sustained expression of PD-1 and expression of LAG-3 are markers of T cell exhaustion.[36] The increased levels of PD-1 and LAG-3 on T cells expressing Hu19-28Z are consistent with a greater susceptibility of T cells expressing this CAR to exhaustion.

Repetitive stimulation of anti-CD19 CAR T cells with CD19 at tumor sites might induce AICD. We assessed the same T cells described in the previous paragraph for AICD after repetitive in vitro stimulation. T cells were stimulated with anti-CD3 on day 0 of culture and transduced on day 1 of culture. The T cells were stimulated with irradiated CD19-K562 cells on days 7 and 10 of culture, and then they were stimulated with NALM6 cells on day 12 prior to annexin V staining on day 13 of culture. We found lower levels of CD19-specific annexin V expression, indicating AICD, among T cells expressing Hu19-CD828Z compared with T cells expressing Hu19-28Z (Figure 6D). At the same time, we assessed Fas ligand (Fas L) expression on the same T cells. We found significant levels of Fas L on T cells transduced with either Hu19-CD828Z or Hu19-28Z, with no statistically significant difference in Fas L expression between T cells expressing the different CARs (Figure S6). Nearly all T cells expressed Fas after repetitive CD19 stimulation regardless of the CAR expressed (not shown).

Human T Cells Expressing Hu19-CD828Z and Hu19-28Z Can Eliminate Tumors of $CD19^+$ Cells In Vivo

We next assessed the in vivo anti-tumor activity of T cells expressing Hu19-CD828Z and Hu19-28Z. Tumors of human $CD19^+$ cells were established in immunocompromised mice. The mice were treated with a single infusion of CAR T cells or left untreated. Tumor growth was substantially inhibited in mice receiving T cells expressing either Hu19-CD828Z or Hu19-28Z. In contrast, untreated mice and mice receiving T cells expressing the SP6-CD828Z negative-control CAR had progressive tumor growth. On day 32 after CAR T cell infusion, tumors were completely eliminated in four of ten mice receiving T cells expressing Hu19-CD828Z, and tumors were completely eliminated in five of ten mice receiving T cells expressing Hu19-28Z. At the end of the experiment on day 49, four of ten mice that received Hu19-CD828Z-expressing T cells were tumor free, and six of ten mice that received Hu19-28Z-expressing T cells were tumor free. There were not statistically significant differences in either tumor sizes or survival when Hu19-CD828Z and Hu19-28Z were compared (Figures 6E and 6F). All mice died when they were sacrificed because of progressive tumors. Mice did not suffer any evident toxicity from the T cells expressing either Hu19-CD828Z or Hu19-28Z. We also assessed T cells expressing either Hu19-CD828Z or Hu19-28Z against disseminated NALM6-GL leukemia cells in NSG mice, and we found that T cells expressing either Hu19-CD828Z or Hu19-28Z were both active against leukemia, but T cells expressing Hu19-CD828Z had less anti-leukemia activity compared with T cells expressing Hu19-28Z (Figures S8 and S9).

DISCUSSION

Anti-CD19 CAR T cells have demonstrated impressive anti-malignancy activity in clinical trials, but some problems, including limited survival of CAR T cells and cytokine-associated toxicity, have also occurred. The clinical effectiveness of anti-CD19 CAR T cells might be increased with improved CAR designs. We have designed novel anti-CD19 CARs with fully human variable regions to limit recipient anti-CAR immune responses, and we have evaluated CARs with hinge and transmembrane regions from either CD8α or CD28. The CD8α sequence is longer than the CD28 sequence and differs from

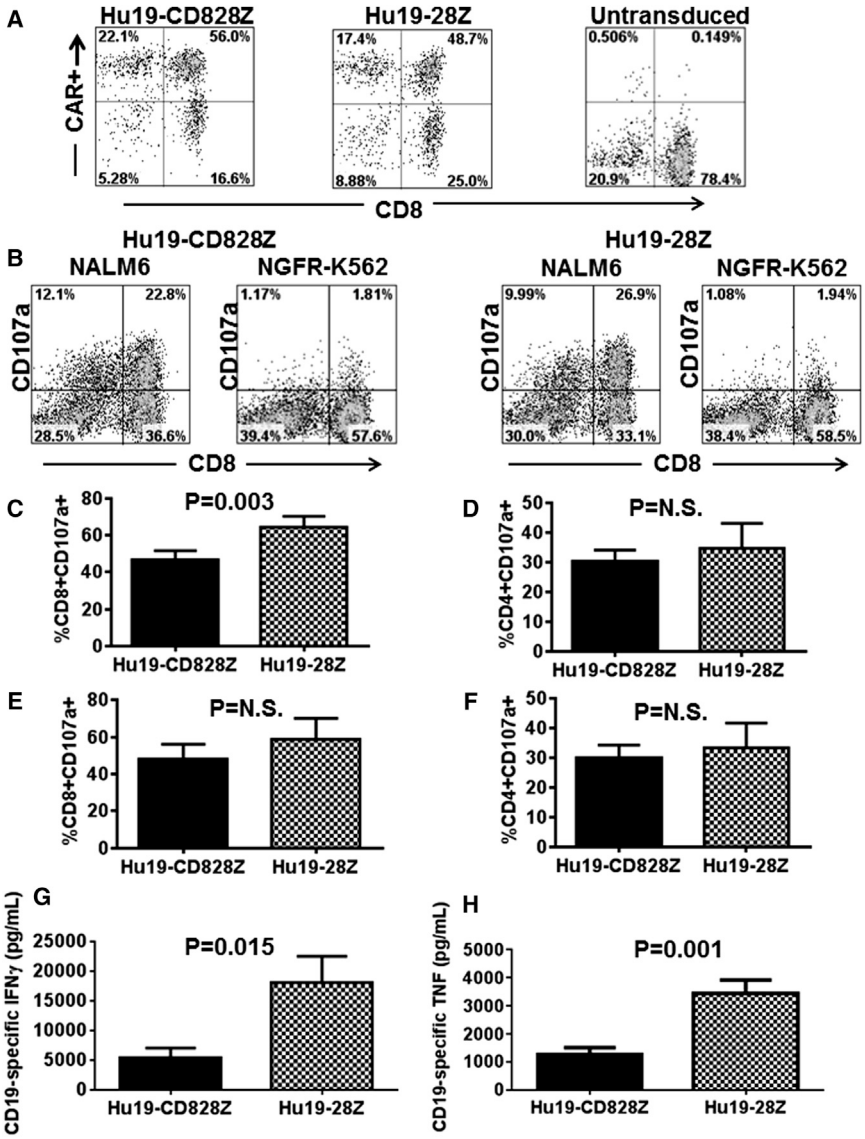

Figure 2. Hu19-CD828Z and Hu19-28Z Were Compared Functionally

(A) T cells from the same donor were transduced with either Hu19-CD828Z or Hu19-28Z. Hu19-CD828Z and Hu19-28Z had similar expression levels on the surface of T cells as measured by protein L staining. Protein L staining of untransduced T cells is also shown. Similar results were obtained in ten different experiments. (B) T cells expressing Hu19-CD828Z or Hu19-28Z were stimulated with either $CD19^+$ NALM6 cells or CD19-negative NGFR-K562 cells, and the CD19-specific increase in CD107a was assessed as a measure of degranulation. Plots are gated on live $CD3^+$ lymphocytes. T cells from five different donors were transduced with either Hu19-CD828Z or Hu19-28Z. (C and D) CD19-specific degranulation of (C) $CD8^+$ T cells or (D) $CD4^+$ T cells expressing the different CARs was compared by measuring CD107a expression in response to NALM6 or NGFR-K562 cells as described in (B). The results shown are the percentages of the T cells expressing $CD8^+$ or $CD4^+$ that degranulated. (E and F) T cells from five different donors were transduced with either Hu19-CD828Z or Hu19-28Z, and CD19-specific degranulation of (E) $CD8^+$ T cells or (F) $CD4^+$ T cells was compared and analyzed as in C except that primary CLL cells were used as the $CD19^+$ target cells. For (C), (D), (E), and (F), CD19-specific degranulation was defined as the fraction of $CD107a^+$ T cells after $CD19^+$ target cell stimulation minus the fraction of $CD107a^+$ T cells after NGFR-K562 stimulation, and CD107a expression was normalized for differences in CAR expression between Hu19-CD828Z and Hu19-28Z. For (C), (D), (E), and (F), CD19-specific degranulation with the different CARs was compared using two-tailed paired t tests, and the mean and SEM of all groups are shown. (G) T cells from five different donors were transduced with either Hu19-CD828Z or Hu19-28Z. The transduced T cells were cultured with either $CD19^+$ NALM6 cells or CD19-negative NGFR-K562 cells overnight, and an ELISA was performed. CD19-specific IFN-γ production was calculated as the IFN-γ production with NALM6 stimulation minus IFN-γ production with NGFR-K562 stimulation. (H) T cells from five different donors were transduced with either Hu19-CD828Z or Hu19-28Z. The transduced T cells were cultured with either $CD19^+$ NALM6 cells or CD19-negative NGFR-K562 cells overnight, and CD19-specific TNF-α production was calculated as the TNF-α production with NALM6 stimulation minus TNF-α production with NGFR-K562 stimulation. For both (G) and (H), the mean and SEM of each group are shown, and cytokine values were normalized to correct for differences in expression of the different CARs on the T cells of each donor. The groups were compared using two-tailed paired t tests.

the CD28 sequence in many other ways (Figure 1B). Compared with a CAR containing hinge and transmembrane regions from CD28, T cells expressing a CAR with hinge and transmembrane regions from CD8α produced lower levels of cytokines and exhibited lower levels of AICD.

T cell activation through either natural T cell receptors or CD3ζ-containing CARs occurs by a process that includes phosphorylation of CD3ζ ITAMs.[34,37] In addition, T cells can undergo apoptosis by a process that is dependent on CD3ζ ITAMs.[37–39] We compared CD3ζ ITAM phosphorylation levels of T cells expressing either Hu19-CD828Z or Hu19-28Z after stimulation of the T cells with either $CD19^+$ target cells or CD19-negative target cells. We found lower levels of CD19-specific CD3ζ ITAM phosphorylation with Hu19-CD828Z compared with Hu19-28Z. This suggested that the activation stimulus of Hu19-CD828Z was weaker than the activation stimulus of Hu19-28Z (Figure 4G). The lower levels of cytokine production and AICD in T cells expressing Hu19-CD828Z compared with T cells expressing Hu19-28Z also suggested that the activation stimulus of Hu19-CD828Z is weaker than the activation stimulus of Hu19-28Z.

To explain the mechanism underlying the differences in CAR function caused by different hinge domains, we investigated the structural

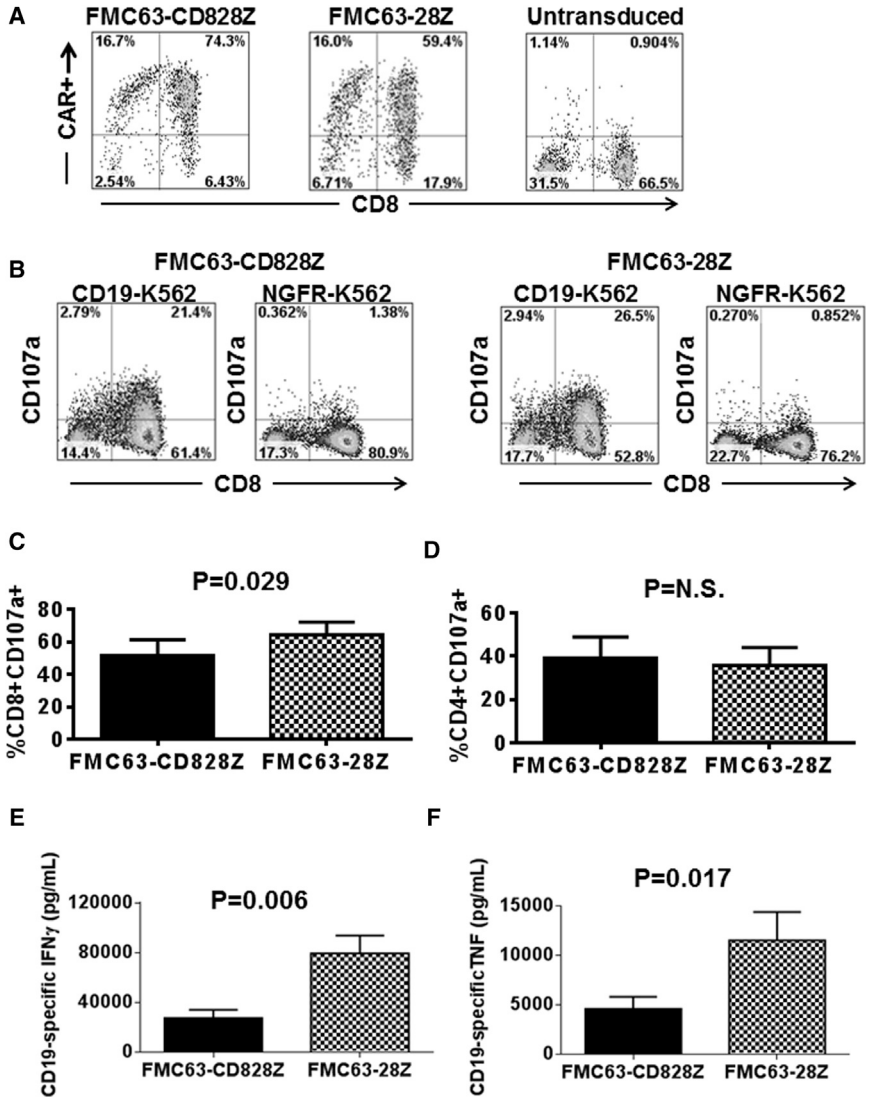

Figure 3. Compared with T Cells Expressing FMC63-CD828Z, T Cells Expressing FMC63-28Z Produced Higher Levels of Inflammatory Cytokines

(A) T cells from the same donor were transduced with either FMC63-CD828Z or FMC63-28Z. The FMC63-CD828Z and FMC63-28Z CARs had similar expression levels on the surface of T cells as measured by anti-fab staining. Anti-fab staining of untransduced T cells is also shown. (B) T cells expressing either FMC63-CD828Z or FMC63-28Z were stimulated with either $CD19^+$ CD19-K562 cells or CD19-negative NGFR-K562 cells. The CD19-specific increase in CD107a was assessed as a measure of degranulation. Plots are gated on live $CD3^+$ lymphocytes. (C) T cells from five different donors were transduced with either FMC63-CD828Z or FMC63-28Z, and CD19-specific degranulation of $CD8^+$ T cells was compared in CD107a degranulation assays that were performed as described in (B). CD19-specific degranulation was calculated as the fraction of $CD8^+CD107a^+$ T cells after CD19-K562 stimulation minus the fraction of $CD8^+CD107a^+$ T cells after NGFR-K562 stimulation. CD107a expression was normalized for differences in CAR expression between FMC63-CD828Z and FMC63-28Z. For (C) and (D), different groups were compared using a two-tailed paired t test, and the mean and SEM of each group are shown. (D) T cells from five different donors were transduced with either FMC63-CD828Z or FMC63-28Z, and CD19-specific degranulation of $CD4^+$ T cells was compared in CD107a degranulation assays that were performed and analyzed as in (C). (E) T cells from five different donors transduced with either FMC63-CD828Z or FMC63-28Z were cultured together with either $CD19^+$ CD19-K562 cells or CD19-negative NGFR-K562 cells overnight. An ELISA was performed, and CD19-specific IFN-γ production was calculated as the IFN-γ production with CD19-K562 stimulation minus IFN-γ production with NGFR-K562 stimulation. (F) T cells from five different donors were transduced with either FMC63-CD828Z or FMC63-28Z. The transduced T cells were cultured together with either CD19-K562 cells or NGFR-K562 cells overnight, and CD19-specific TNF-α production was calculated as the TNF-α production with CD19-K562 stimulation minus TNF-α production with NGFR-K562 stimulation. For both (E) and (F), the mean and SEM of each group is shown, and cytokine values were normalized to correct for differences in expression of the different CARs on the T cells of each donor. Also for (E) and (F), the groups were compared using two-tailed paired t tests.

information known about CD8α and CD28. A comparison of the crystal structures of the extracellular domains of CD28 and CD8α reveal putative differences that the hinge domains of CD8α and CD28 confer upon each respective homodimerization interface. As seen in a structural model of CD28 (Figure 7A), the residues that comprise the hinge domain of the CD28 homodimer span the dimerization interface and play an important role in the formation of CD28 homodimers.[40] In structural studies of the CD8α homodimer, a 141-amino acid construct was expressed comprising the N-terminal 114-amino acid immunoglobulin domain and a 27-amino acid C-terminal tail.[41] These studies revealed that the tail of this construct was not ordered, which suggested flexibility of this region. In contrast to the hinge derived from CD28, the hinge from this region of CD8α is less likely to be located at the dimerization interface, with the C-terminal residues in the structure being apart (Figure 7B). This suggests that the hinge region of CD8α proximal to the scFv domain does not interact in the setting of a CAR dimer. Further, the extracellular stalk of CD8α is heavily glycosylated and negatively charged, which also reduces the propensity for self-association.[41]

We hypothesize that CAR molecules with either a CD28 or CD8α hinge domain exist in equilibrium between monomeric and homodimeric states. On the basis of the contributions from the hinge domains that are resolved in the crystal structures, we hypothesize that a CD28 hinge is more likely to push the equilibrium toward the dimeric state compared with a CD8α hinge. We further hypothesize that the CAR activation stimulus may be stronger with a CD28 hinge compared with a CD8α hinge because of the greater propensity

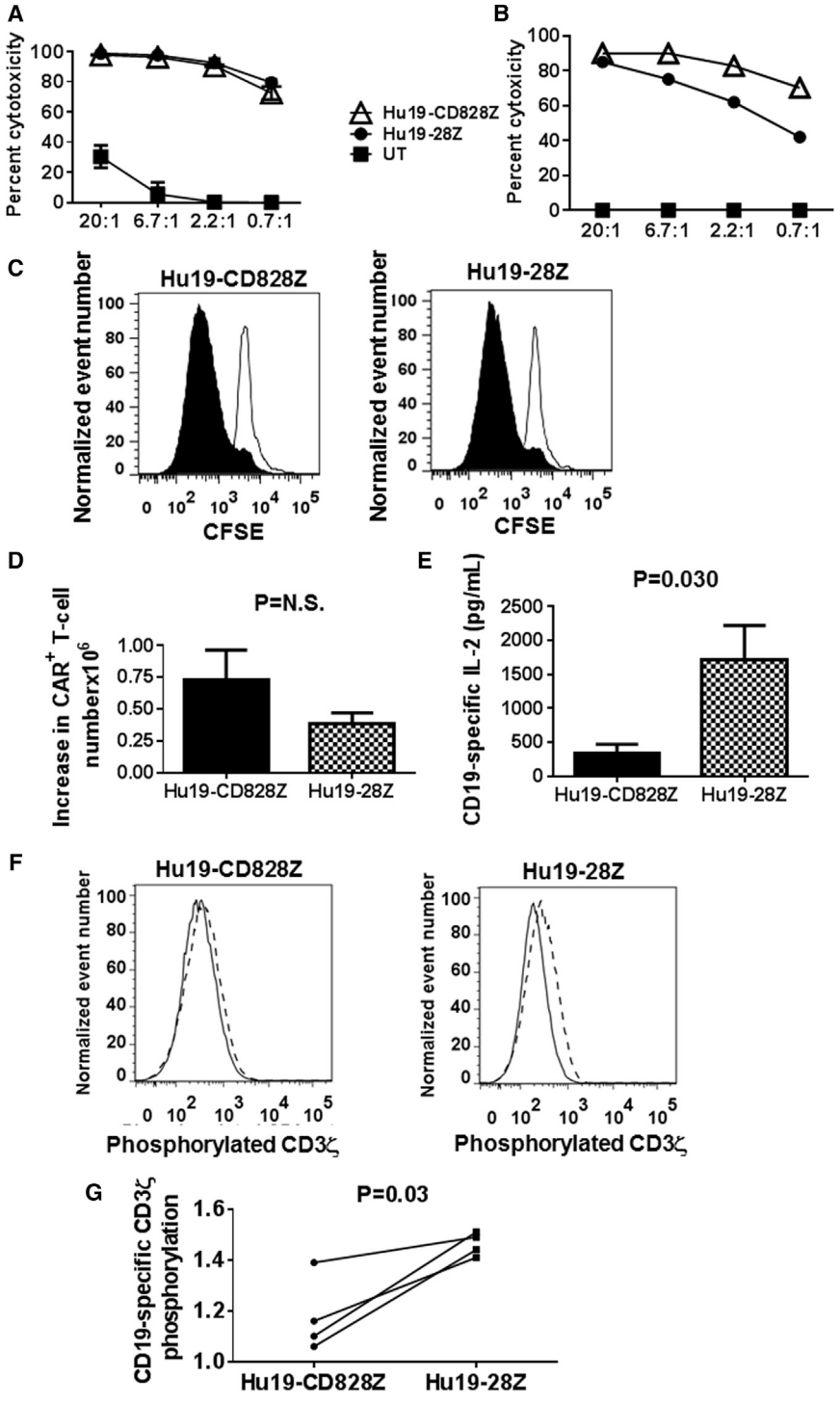

Figure 4. CD3ζ Phosphorylation, T Cell Proliferation, and IL-2 Release with Hu19-CD828Z versus Hu19-28Z

(A) T cells from the same donor were transduced with either Hu19-CD828Z or Hu19-28Z or left untransduced, and a 4 hr cytotoxicity assay was performed with Toledo $CD19^+$ lymphoma cell line cells as target cells. Error bars represent SEM. (B) Primary chronic lymphocytic leukemia cells were used as target cells in a 4 hr cytotoxicity assay comparing Hu19-CD828Z and Hu19-28Z. The numbers on the x-axes in both (A) and (B) are the effector to target ratios. (C) CFSE-labeled T cells from the same donor expressing either Hu19-CD828Z or Hu19-28Z were cultured for 4 days with irradiated CD19-K562 (filled histograms) or NGFR-K562 (open histograms). The degree of proliferation was similar for T cells expressing the different CARs; this was a representative example of six different donors. The plots are gated on live $CD3^+CAR^+$ lymphocytes. (D) T cells from six different donors were transduced with either Hu19-CD828Z or Hu19-28Z. The T cells were cultured, transduced, and labeled with CFSE as in (C). The mean increases in the numbers of CAR^+ T cells during the 4-day culture are shown for T cells expressing each CAR. The increases in CAR T cell numbers were calculated as the number of CAR^+ T cells on day 4 of culture minus the number of CAR^+ T cells at the start of the cultures. Error bars represent SEM. (E) T cells from six different donors expressing either Hu19-CD828Z or Hu19-28Z were cultured together with either $CD19^+$ NALM6 cells or CD19-negative NGFR-K562 cells overnight, and an ELISA for IL-2 was performed. CD19-specific IL-2 production was calculated as the IL-2 production with NALM6 stimulation minus IL-2 production with NGFR-K562 stimulation. The mean and SEM of each group are shown. IL-2 values were normalized to correct for differences in expression of the different CARs on the T cells of each donor. The groups were compared using a two-tailed paired t test. (F) T cells from four patients were transduced with either Hu19-CD828Z or Hu19-28Z. The cells were sorted to obtain pure populations of CAR^+ T cells expressing either Hu19-CD828Z or Hu19-28Z. The T cells were stimulated with either $CD19^+$ NALM6 cells or CD19-negative NGFR-K562 cells. The level of phosphorylation of tyrosine-142 in an immune receptor tyrosine-based activation motif (ITAM) of the CD3ζ molecules of the T cells (CD19-specific CD3ζ phosphorylation) was then assessed by intracellular flow cytometry. Representative examples of the flow cytometry staining for Hu19-CD828Z and Hu19-28Z are shown. The solid-line histograms show the level of phosphorylated CD3ζ on T cells stimulated with NGFR-K562. The histograms with dashed borders show the level of phosphorylated CD3ζ on T cells stimulated with NALM6. (G) CD19-specific CD3ζ phosphorylation of T cells from four patients was calculated by dividing the median fluorescence intensity of phosphorylated CD3ζ tyrosine-142 staining after NALM6 stimulation by the median fluorescence intensity of phosphorylated CD3ζ tyrosine-142 staining after NGFR-K562 stimulation. The level of CD19-specific CD3ζ phosphorylation was lower in T cells expressing Hu19-CD828Z than in T cells expressing Hu19-28Z. Groups were compared with a two-tailed paired t test.

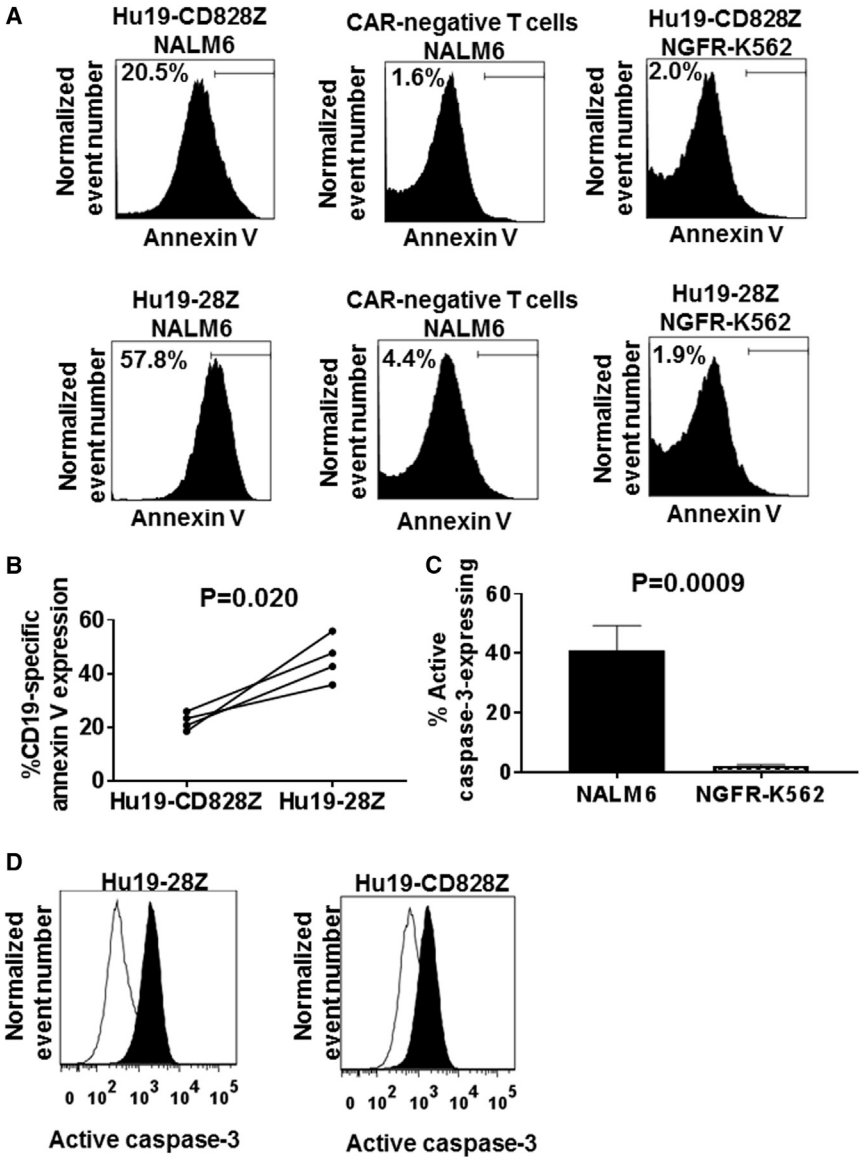

Figure 5. Levels of Activation-Induced Cell Death Were Lower in Hu19-CD828Z-Expressing T Cells Than in Hu19-28Z-Expressing T Cells

(A) T cells from the same donor were transduced with either Hu19-CD828Z or Hu19-28Z and cultured overnight with either $CD19^+$ NALM6 cells or CD19-negative NGFR-K562 cells. The cells were then stained with annexin V to detect apoptotic T cells. The top row of plots shows T cells transduced with Hu19-CD828Z. The bottom row of plots shows T cells transduced with Hu19-28Z. These T cell cultures contained both CAR-expressing T cells and CAR-negative T cells. The top label above each plot gives the status of CAR expression of the T cells shown on the plot. The lower label above each plot gives the target cell that the T cells were cultured with. After culture with $CD19^+$ NALM6 cells, a smaller fraction of Hu19-CD828Z-expressing T cells than Hu19-28Z-expressing T cells expressed annexin V. (B) T cells from 4 donors were transduced with either Hu19-CD828Z or Hu19-28Z and cultured overnight with either NALM6 cells or NGFR-K562 cells. Annexin V staining assays were performed as described in (A). Compared with T cells expressing Hu19-28Z, T cells expressing Hu19-CD828Z had a lower percentage CD19-specific annexin V expression. The percentage CD19-specific annexin V expression was calculated as the percentage $CD3^+$ CAR^+ annexin V^+ cells with NALM6 stimulation minus the percentage $CD3^+$ CAR^+ annexin V^+ cells with NGFR-K562 cell stimulation. Paired results of T cells from each patient transduced with either Hu19-CD828Z or Hu19-28Z are connected by a line. Experiments were conducted with cells from four different patients. Comparison was made using a two-tailed paired t test. (C) CAR T cells were stimulated with either $CD19^+$ NALM6 cells or CD19-negative NGFR-K562 cells overnight, and the CAR T cells were assessed for active caspase-3 expression by intracellular flow cytometry. Results for cells from six different donors are included. For each donor, T cells transduced with Hu19-CD828Z and T cells expressing Hu19-28Z were included on this graph, so a total of 12 different cell T cell populations were included. For all 12 T cell populations, active caspase-3 levels increased with CD19-K562 stimulation compared with NGFR-K562 stimulation. The paired two-tailed t test was used. Error bars represent SEM. (D) Active caspase-3 expression was higher in CAR T cells cultured overnight with $CD19^+$ NALM6 cells (filled histograms) than in T cells cultured with NGFR-K562 cells (open histograms). For both (C) and (D), live $CD3^+CAR^+$ T cells were assessed.

of CARs with a CD28 hinge to dimerize. This hypothesis is in accordance with the work of others showing that aggregation of CD3ζ molecules promotes T cell activation.[42,43] If this hypothesis is true, the stronger activation stimulus could lead to the observed functional differences in T cells expressing Hu19-CD828Z versus Hu19-28Z, such as the differences in cytokine production and AICD. As we learn more about CAR functionality and the importance of hinge domains on CAR function, it is possible that optimal hinges from either CD28 or CD8α could be selected for different indications or target antigens.

Previously reported anti-CD19 CARs have incorporated murine scFvs.[7,8,10–13,15,21] Compared with CARs with murine scFvs, a CAR with a fully human scFv should be less likely to elicit anti-CAR immune responses; however, the risk of anti-CAR immune responses will not be completely eliminated by use of fully human variable regions. Amino acid sequences not naturally expressed in humans are present at junctions between the different components of the CAR, and the linker that connects the light chain and heavy chain variable regions is an artificial sequence. Immunogenic sequences are also potentially in idiotypic epitopes of the variable regions.[44] Any foreign protein could potentially elicit an anti-CAR immune response, so efforts should be made to limit non-human CAR amino acid sequences as much as possible. Compared with the FMC63-CD828Z CAR that contains a murine scFv, the human Hu19-CD828Z CAR

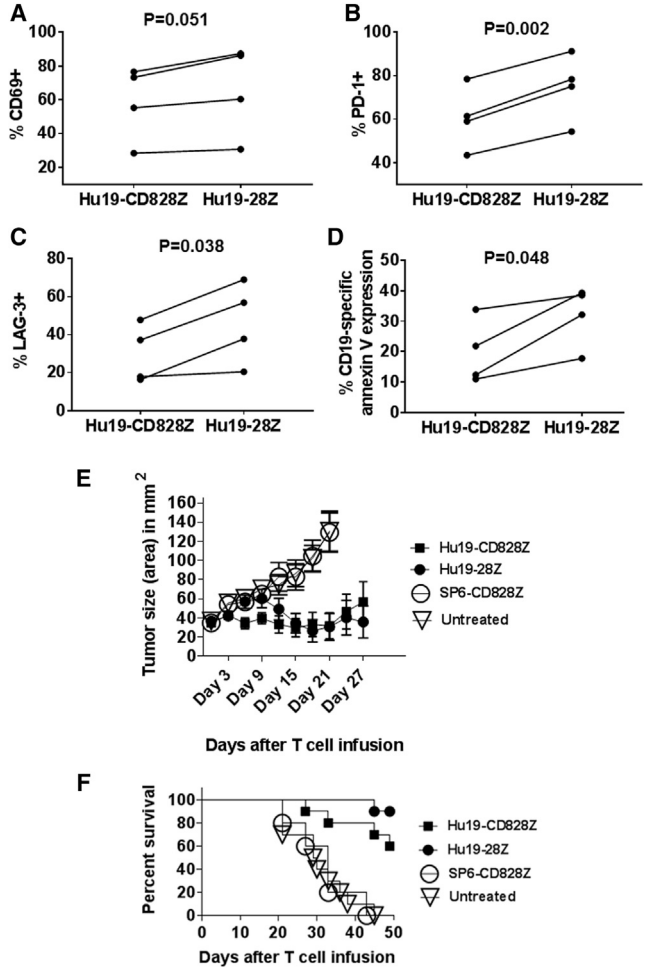

Figure 6. After In Vitro Stimulation with CD19$^+$ Target Cells, T Cells Expressing Hu19-CD828Z Undergo Less AICD Than T Cells Expressing Hu19-28Z, and T Cells Expressing Either Hu19-CD828Z or Hu19-28Z Can Eliminate Established Tumors in Mice

(A–C) T cells from four different donors were transduced with either Hu19-CD828Z or Hu19-28Z. The T cells were stimulated with irradiated CD19$^+$ CD19-K562 cells on day 7 and day 10 after initiation of the cultures. On day 12 after culture initiation, flow cytometry was performed to measure CD69 (A), PD-1 (B), and LAG-3 (C) expression on CD3$^+$CAR$^+$ T cells. (D) T cells from 4 different donors were transduced with either Hu19-CD828Z or Hu19-28Z. The T cells were stimulated with irradiated CD19-K562 cells on day 7 and day 10 after initiation of the cultures. On day 12 after culture initiation, the T cells were cultured overnight with either NALM6 or NGFR-K562 target cells and annexin V staining was conducted. The percentage CD19-specific annexin V expression was calculated as the percentage CD3$^+$ CAR$^+$ annexin V$^+$ cells with NALM6 stimulation minus the percentage CD3$^+$ CAR$^+$ annexin V$^+$ cells with NGFR-K562 stimulation. For (A)–(D), paired results of T cells from each of four patients are connected by a line. Comparison was made using a two-tailed paired t test. (E) NALM6 tumors were established in immunocompromised NSG mice. The mice then received infusions of 8 million T cells transduced with Hu19-CD828Z or Hu19-28Z or the negative-control CAR SP6-CD8Z. A fourth group of mice was left untreated. Tumors were measured every 3 days in a blinded manner. Combined results of two separate experiments that used cells from two different human donors are shown. There was a total of ten mice in each group except the SP6-CD828Z group, which had five mice. The graphs show the mean tumor size ± SEM for each time point. (F) Survival of the same mice as in Figure 5E is shown. By the log rank test, there was a statistically significant difference in survival between mice receiving T cells that expressed Hu19-CD828Z versus SP6-CD828Z ($p = 0.003$). There was also a statistically significant difference in survival between mice receiving T cells that expressed Hu19-28Z versus SP6-CD828Z ($p < 0.0001$). There were statistically significant differences in survival between mice receiving T cells expressing either Hu19-CD828Z ($p = 0.0005$) or Hu19-28Z ($p < 0.0001$) versus untreated mice. There was not a statistically significant difference in survival by the log rank test when mice receiving T cells expressing Hu19-CD828Z or Hu19-28Z were compared ($p = 0.12$).

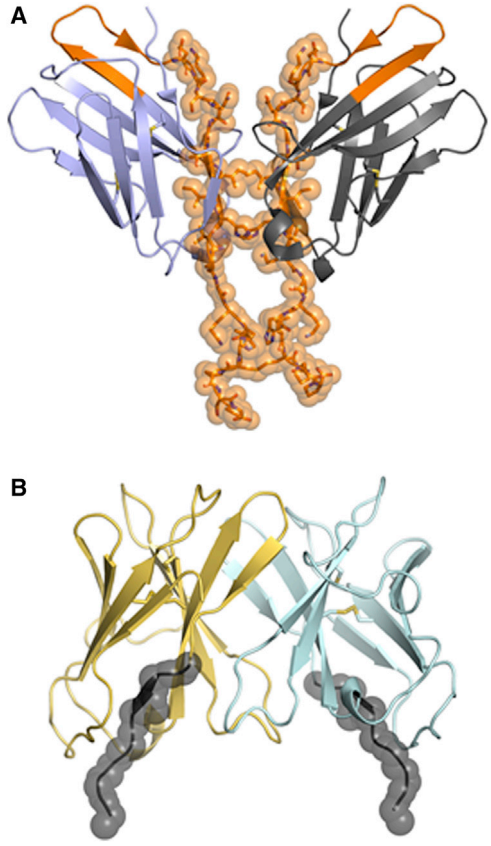

Figure 7. Hypothesized Models of the CD28 and CD8a Hinge Regions

(A) The immunoglobulin domains of the CD28 homodimeric structure are shown in blue and gray. The C-terminal tail was modeled to add additional residues on the basis of high sequence identity and structural homology with CTLA-4. The residues interacting at the dimer interface within the CAR hinge are shown as orange sticks and spheres. (B) The immunoglobulin domains of the CD8α homodimer are shown in yellow and cyan. The residues included in the hinge domain are shown in black with spheres (FVPVFLPA). The region of the CD8α hinge domain is not hypothesized to strongly contribute to dimerization.

exhibited strong and specific recognition of CD19$^+$ target cells, so we concluded that the Hu19 scFv was an appropriate anti-CD19 scFv to include in CARs (Table 2).

In addition to recipient anti-CAR immune responses, another potential mechanism of in vivo elimination of CAR T cells is AICD.[28–32] The AICD that CAR T cells exhibited in our experiments was likely

dependent on the caspase pathway, as active caspase-3 was consistently increased when CAR T cells were stimulated with $CD19^+$ target cells in all of our experiments that measured active caspase-3 levels (Figure 5C). The Hu19-CD828Z CAR with CD8α hinge and transmembrane regions underwent less AICD than the Hu19-28Z CAR with CD28 hinge and transmembrane regions (Figures 5A and 5B). Genetic modification of CAR T cells with an aim of reducing AICD might be an effective approach to increase CAR T cell persistence in vivo.

There was not a statistically significant difference in proliferation as measured by CFSE dilution (Figure 4C) or increase in T cell number (Figure 4D) when Hu19-CD828Z CAR T cells were compared with Hu19-28Z CAR T cells. Because of the lower levels of AICD in Hu19-CD828Z CAR T cells, these findings might be somewhat unexpected. These results could be due to the much higher level of IL-2 production by Hu19-28Z CAR T cells (Figure 4E). This high level of IL-2 production by Hu19-28Z CAR T cells might be one factor promoting in vitro proliferation by Hu19-28Z CAR T cells, while other factors such as high levels of AICD might limit the increase in the number of T cells expressing this CAR. IL-2 production might be a particularly important factor in vitro when no exogenous cytokines were added to the culture media as was the case in our proliferation experiments.

In our past clinical experience, we administered T cells expressing the FMC63-28Z CAR, which contained hinge and transmembrane regions from CD28. T cells expressing FMC63-28Z usually persisted in the blood of patients for less than 2 months.[10,14,19,45] Blood CAR^+ cell numbers in patients who received T cells expressing the FMC63-28Z CAR usually rose to a peak within the first 2 weeks after infusion and then rapidly decreased.[10,14,19] It is certainly plausible that AICD was a major mechanism of elimination of these cells because we have shown that T cells expressing the FMC63-28Z CAR underwent substantial AICD in vitro (Figure S7).

We found a reduced level of AICD in Hu19-CD828Z compared with Hu19-28Z, which favored selecting the Hu19-CD828Z CAR for further testing and development. Importantly, we showed that T cells expressing Hu19-CD828Z underwent less AICD compared with T cells expressing Hu19-28Z after only 1 stimulation with $CD19^+$ target cells (Figure 5B) and after multiple in vitro stimulations with $CD19^+$ target cells (Figure 6D). Anti-CD19 CAR T cells are likely undergo repetitive stimulation with CD19 in vivo, so resistance to AICD after multiple antigen exposures is an important attribute for CAR-expressing T cells. After repetitive in vitro exposure to CD19, we found lower levels of PD-1 and LAG-3 on T cells expressing Hu19-CD828Z compared with T cells expressing Hu19-28Z (Figures 6B and 6C). These markers are associated with T cell exhaustion.[46]

Cytokine-mediated toxicity is a significant clinical problem limiting CAR T cell therapies.[9,15,16,33] We have shown in prior clinical trials that patients receiving T cells expressing the FMC63-28Z CAR often experienced substantial toxicity that was associated with increased serum levels of inflammatory cytokines.[9,10,19] If cytokine-mediated toxicity of CAR T cells could be reduced, higher doses of CAR T cells could potentially be administered. Increased CAR T cell doses might improve anti-malignancy efficacy because most murine models indicate that higher doses of adoptively transferred T cells are more effective than lower doses of T cells at eliminating tumors.[47,48] Perhaps the most important current goal of the CAR field is to find approaches that reduce the toxicity of CAR T cells without substantially impairing their anti-malignancy efficacy. We found that cytokine production by Hu19-CD828Z-expressing T cells was lower than cytokine production by Hu19-28Z-expressing T cells, but in vivo anti-tumor activity of T cells expressing the two CARs was similar. The reduced cytokine production by Hu19-CD828Z-expressing T cells compared with Hu19-28Z-expressing T cells is a potential clinical advantage for Hu19-CD828Z and possibly the most important finding of this study.

The results of our solid tumor experiments showed no statistically significant difference in the ability of Hu19-CD828Z versus Hu19-28Z to eliminate tumors (Figures 6E and 6F). Despite the reduced cytokine production of T cells expressing Hu19-CD828Z versus T cells expressing Hu19-28Z, T cells expressing Hu19-CD828Z can eliminate malignant cells from mice. Our goal is to find a CAR that has the best efficacy to toxicity ratio in humans. Because toxicity is such a significant clinical problem with CAR T cell therapies,[10,15–17,49] it is possible that the better overall CAR for clinical use might be a CAR that is associated with less toxic cytokine release even if this CAR has slightly less anti-malignancy activity in NSG mice. We hypothesize that Hu19-28Z has an advantage over Hu19-CD828Z in NSG mice because T cells expressing Hu19-28Z produce much higher levels of cytokines such as IL-2. For anti-malignancy activity, the importance of cytokines produced by CAR T cells is possibly greater when NSG mice receive human CAR T cells than when humans receive human CAR T cells. For the important cytokine IL-15, murine IL-15 is much less effective than human IL-15 at inducing proliferation of human T cells.[50] Any anti-malignancy advantage that Hu19-28Z has over Hu19-CD828Z in NSG mice because of the greater cytokine production by T cells expressing Hu19-28Z might be reduced or absent in humans because human serum contains important cytokines such as IL-15 and IL-7 at the time of CAR T cell infusion, which might make production of cytokines such as IL-2 by CAR T cells less important.[49]

Importantly, there was not a statistically significant difference in eradication of solid tumors from mice when T cells expressing either Hu19-CD828Z or Hu19-28Z were compared, while levels of potentially toxic cytokine release and AICD were decreased with Hu19-CD828Z versus Hu19-28Z. T cells expressing Hu19-CD828Z were active against disseminated leukemia in a murine model, but Hu19-CD828Z was modestly inferior to Hu19-28Z at eliminating disseminated leukemia (Figures S8 and S9). We observed no difference in toxicity in mice receiving the T cells expressing the different CARs, but this is not surprising because we have found that mice seem to

be quite resistant to CAR T cell toxicity. In our experience, mice have had no apparent toxicity after receiving weight-based CAR T cell doses that were much higher than doses that caused severe toxicity in humans.[9,10,38,51] We have designed and constructed novel anti-CD19 CARs with fully human variable regions, and we have shown that the hinge and TM regions of CARs can affect CAR T cell cytokine production and AICD susceptibility. Compared with T cells expressing Hu19-28Z, T cells expressing Hu19-CD828Z exhibited lower levels of potentially harmful cytokine production and AICD. T cells expressing either Hu19-CD828Z or Hu19-28Z had similar ability to eradicate tumors in vivo; therefore, we selected Hu19-CD828Z for testing in a phase I clinical trial. Early results from this trial confirm that Hu19-CD828Z has anti-lymphoma activity in humans; 9 of 12 patients treated with T cells expressing this CAR have obtained objective anti-lymphoma responses (Brudno et al., 2016, American Society of Hematology, abstract).

MATERIALS AND METHODS

Construction of Plasmids Encoding Anti-CD19 CARs

We designed anti-CD19 CARs containing variable region sequences of a fully human antibody called 47G-4.[52] A scFv designated Hu19 was designed with the following sequence from 5′ to 3′: human CD8α signal sequence, light chain variable region, a linker peptide[44] (GSTSGSGKPGSGEGSTKG), heavy chain variable region. A DNA sequence encoding a CAR with the following components from 5′ to 3′ was designed: Hu19 scFv, part of the extracellular region and the transmembrane region of the human CD8α molecule (Figure 1B), the cytoplasmic portion of the human CD28 molecule, and the cytoplasmic part of the human CD3ζ molecule. The DNA sequence was synthesized (Thermo Fisher Scientific/Invitrogen). We designated this CAR Hu19-CD828Z. By using standard methods, we replaced the coDMF5 portion of the pRRLSIN.cPPT.MSCV.coDMF5.oPRE[53] lentiviral vector plasmid with the Hu19-CD828Z CAR sequence. We designated the resulting plasmid LSIN-Hu19-CD828Z. The sequences of CD8α, CD28, and CD3ζ were obtained from the National Center for Biotechnology Information website (http://www.ncbi.nlm.nih.gov). Guidance regarding the portions of each molecule to include in the CARs was obtained from prior work.[54]

The Hu19-28Z CAR had this sequence from 5′ to 3′: the Hu19 scFv, part of the extracellular region of human CD28, all of the transmembrane and cytoplasmic regions of CD28, and the cytoplasmic part of CD3ζ. The LSIN-Hu19-28Z plasmid has the same sequence as LSIN-Hu19-CD828Z except for the replacement of the CD8α hinge and transmembrane region in LSIN-Hu19-CD828Z with hinge and transmembrane regions from CD28 in LSIN-Hu19-28Z.

The SP6 scFv recognizes the hapten 2, 4, 6-trinitrobenzenesulfonic acid.[5] We constructed a lentiviral plasmid encoding a CAR with the SP6 scFv designated LSIN-SP6-CD828Z, and we used it as a negative control as previously described.[51]

Construction of the gammaretroviral MSGV-FMC63-28Z plasmid encoding the FMC63-28Z anti-CD19 CAR has already been described.[54] A DNA fragment encoding part of the extracellular region and all of the transmembrane region of the human CD8α molecule and the cytoplasmic portion of the CD28 molecule was synthesized by Thermo Fisher Scientific/Invitrogen. This fragment was used to replace the entire CD28 portion of the MSGV-FMC63-28Z plasmid to form FMC63-CD828Z.

Patient Samples and Cell Lines

Peripheral blood mononuclear cells (PBMCs) and chronic lymphocytic leukemia samples were obtained from hematologic malignancy patients who were enrolled on National Cancer Institute, institutional review board-approved protocols. In experiments that used primary CLL cells as target cells, unmanipulated PBMC from patients with CLL were used. We previously transduced K562 cells to express CD19 (CD19-K562) or low-affinity nerve growth factor (NFGR-K562).[54] The NGFR-K562 cells served as CD19-negative control cells. $CD19^+$ NALM6 cells (acute lymphoid leukemia from DSMZ) were used. The following CD19-negative human cell lines were used: A549 (lung carcinoma, ATCC), CCRF-CEM (T cell leukemia, ATCC), MDA231 (breast carcinoma, ATCC), 293T-17 (embryonic kidney cells, ATCC), TC71 (Ewing's sarcoma, a kind gift of Dr. M. Tsokos, National Cancer Institute).

T Cell Culture

PBMCs were thawed and washed in T cell medium that consisted of AIM V medium (Invitrogen) plus 5% AB serum (Valley Biomedical), 100 U/mL penicillin, and 100 μg/mL streptomycin. Prior to transductions, PBMC were suspended at a concentration of 1×10^6 cells/mL in T cell medium plus 50 ng/mL of the anti-CD3 monoclonal antibody OKT3 (Ortho) and 300 IU/mL of IL-2. After transductions, T cells were maintained in T cell medium plus IL-2.

Gammaretroviral Transductions

To produce replication-incompetent gammaretroviruses, packaging cells were transfected with plasmids encoding CARs along with a plasmid encoding the RD114 envelope protein as previously described.[54] Gammaretroviral transduction of T cells was performed as previously described 2 days after initiation of T cell cultures.[54]

Lentiviral Transductions

To produce lentivirus-containing supernatant, 293T-17 cells (ATCC) were transfected with the following plasmids as detailed previously: pMDG (encoding the vesicular stomatitis virus envelope), pMDLg/pRRE (encoding gag and pol), pRSV-Rev (encoding Rev), and the appropriate CAR-encoding plasmid.[51]

Twenty-four hours after the T cell culture initiation, lentivirus vector and protamine sulfate were added to the T cell cultures. The cells were cultured with the lentivirus vector for 48 hr, and then they were washed and returned to culture in T cell medium.

CAR Detection on Transduced T Cells

Biotin-labeled polyclonal goat anti-mouse-$F(ab)_2$ antibodies (anti-Fab, Jackson Immunoresearch) were used to detect the FMC63 scFv

as previously described.[54] In experiments that evaluated the human Hu19 scFv, cell-surface CAR expression was detected with Biotin-labeled protein L (GenScript). The percentage of CAR-expressing (CAR^+) T cells was calculated as the percentage of T cells in CAR-transduced cultures that stained with the anti-Fab antibodies or protein L minus the percentage of identically cultured untransduced T cells from the same donor staining with anti-Fab or protein L.

IFN-γ, TNF-α, and IL-2 ELISAs

One hundred thousand effector T cells were combined with 100,00 target cells in each well of 96-well plates. The plates were incubated at 37°C for 18-20 hr. Following the incubation, ELISAs were performed using standard methods (Thermo Fisher Scientific/Pierce). In some experiments, antigen-specific cytokine release was calculated by subtracting cytokine release by T cells cultured with NGFR-K562 negative-control target cells from cytokine release by T cells cultured with $CD19^+$ target cells. When two or more CARs were compared, cytokine release was normalized for CAR expression by dividing the cytokine levels by the fraction of T cells expressing a given CAR.

Cytotoxicity Assay, CD107a Degranulation, and Proliferation

Cytotoxicity assays, CD107a degranulation, and carboxyfluorescein succinimidyl ester (CFSE; Thermo Fisher Scientific/Invitrogen) proliferation assays were conducted as previously described.[51,54,55] CD107a expression was normalized for CAR expression by dividing the fraction of $CD107a^+$ T cells by the fraction of T cells expressing a given CAR.

Phosphorylated CD3ζ Staining

CAR-transduced T cells were stained with protein L and CD3. Cells that were positive for CD3 and protein L were sorted by using either a BD Influx cell sorter or a BD FACsAria cell sorter (BD Biosciences). The T cells were cultured overnight in IL-2-containing media. After overnight culture, 1×10^6 $CD3^+L^+$ cells were stimulated with 0.5×10^6 NALM-6 or NGFR-K562 target cells. To initiate stimulation, cells were centrifuged at $300 \times g$ for 30 s and incubated at 37°C for 8–10 min. Stimulation was stopped, and cells were fixed by adding 4 mL of PhosFlow Lyse/Fix Buffer (BD Biosciences) and incubating at 37°C for 10 min. The cells were washed then permeabilized by adding 3 mL of PhosFlow Perm Buffer III (BD Biosciences) and incubating on ice for 20 min. Cells were then stained for 20 min at room temperature with anti-CD3 and a PE-conjugated antibody that binds only to phosphorylated tyrosine 142 in an ITAM of the CD3ζ molecule (BD Biosciences).

Annexin V Staining

CAR-transduced T cells were incubated overnight in 24-well plates with either NALM6 or NGFR-K562 target cells with 1.5×10^6 T cells and 1×10^6 target cells in each well. After overnight incubation, cells were stained with protein L and CD3. The cells were washed twice with PBS, re-suspended in annexin V binding buffer (BD Biosciences), and incubated with allophycocyanin-conjugated annexin V (BD Biosciences) and 7AAD (BD Biosciences) for 15 min at room temp. The cells were immediately analyzed by flow cytometry.

Active Caspase-3 Staining

We incubated 1.5×10^6 CAR T cells overnight with 1×10^6 NALM-6 or NGFR-K562 cells. Cells were then stained with protein L to detect CAR^+ T cells and stained for CD3. After washing twice, the cells were fixed and permeabilized with 1 mL of BD Cytofix/Cytoperm (BD Biosciences) and stained with anti-active caspase-3-PE (BD Biosciences).

In Vitro Multi-stimulation

PBMC were cultured and transduced as described under T Cell Culture and Lentiviral Transductions above. On day 7 after T cell culture initiation (day 7), Hu19-28z and Hu19-CD828z CAR T cells were suspended in AIM V with no IL-2 and were incubated at 37°C with irradiated CD19-K562 at a ratio of 1:1 for 3 days. Three days later, on day 10 of culture, CAR-T cells were counted and incubated with freshly irradiated CD19-K562 at a 1:1 ratio for another 2 days. On day 12 of overall culture, CAR T cells were stained with the cell surface markers or were set up for an annexin V assay. The annexin V assay consisted of an overnight culture with NALM6 or NGFR-K562 target cells followed by staining with anti-CD3, protein L, and annexin V staining as described under Annexin V Staining.

Murine Solid Tumor Experiments

NSG mice (NOD.Cg-*Prkdc*^{scid} *Il2rg*^{tm1Wjl}/SzJ) (Jackson Laboratory) were used. Mice received intradermal injections of 4×10^6 NALM6 cells. The cells were suspended in a solution of 50% PBS and 50% Matrigel (Corning). Tumors were allowed to grow for 6 days, and then the mice received intravenous infusions of 8×10^6 human T cells that were transduced with either LSIN-Hu19-28Z or LSIN-Hu19-CD828Z. Tumors were measured with calipers every 3 days. The longest length and the length perpendicular to the longest length were multiplied to obtain the tumor size (area) in square millimeters. When the longest length reached 15 mm, mice were sacrificed. Animal studies were approved by the National Cancer Institute Animal Care and Use Committee.

Murine Disseminated Leukemia Experiments

Mice were intravenously injected with 2×10^6 NALM6-GL via the retro-orbital route. After 3 days, mice were infused with 4×10^6 Hu19-28z or Hu19-828z total T cells. Any difference in the percentage of CAR expressing T cells between the two CARs was normalized by adjusting the total number of T cells infused for one group. Bioluminescence images of the mice were taken on the day of CAR T cell infusion and every 4 days thereafter. Imaging was done as follows: mice were intraperitoneally injected with 15 mg/mL of luciferin (Goldbio) in 200 μL of PBS. Bioluminescence images were taken 10 min after luciferin injection, while the mice were under anesthesia with 3% isoflurane. Images were captured using Xenogen IVIS Imaging System with Living Imaging software. Ventral images were captured at 30 s exposures on a 24 cm field of view and at binning factor 4. Bioluminescence was quantified through region of interest analysis over the whole mouse excluding the tail. Bioluminescence signals were given as photons per second per square centimeter per steradian.

Flow Cytometry and Statistics

In all flow cytometry experiments, acquisition was performed with either LSR II or LSRFortessa (both from BD Biosciences) flow cytometers, and analysis was performed with FlowJo (TreeStar). Statistical analyses were performed with Graph Pad Prism version 6. Cell cultures were stained during in vitro multi-stimulation experiments with cell surface markers LAG-3-eFlour450 (eBioscience), PD-1-BV711 (Biolegend), CD57-FITC, TIM-3-APC, CD25-FITC, Fas-L-V450, Fas-APC, CD69-FITC, CD45RA-FITC, CCR7-APC, and CD62L-V450 (BD Biosciences) for flow cytometry analysis before and after multi-stimulation with target cells in vitro.

Molecular Modeling and Visualization

Structural coordinates for CD28 (PDB: 1YJD) and CD8α (PDB: 1CD8) were obtained from the Protein Data Bank (http://www.rcsb.org).[56] Molecular visualization and figure generation was performed using PyMOL (Schrodinger). Additional residues were modeled into the CD28 structure on the basis of sequence and structural alignment with a CTLA-4 structure (PDB: 3BX7). Additional energy minimization was performed with Molecular Operating Environment (MOE) version 2013.08 (Chemical Computing Group).

SUPPLEMENTAL INFORMATION

Supplemental Information includes nine figures and six tables and can be found with this article online at http://dx.doi.org/10.1016/j.ymthe.2017.07.013.

AUTHOR CONTRIBUTIONS

L.A. performed and planned experiments, analyzed data, and participated in writing the paper; M.P., C.G., V.S., and S.Y. performed experiments and edited and approved the manuscript; J.J.W.W. and S.A.S. devised the structural model in Figure 7, analyzed data, and edited and approved the manuscript; J.N.K. devised experiments, planned the project, performed experiments, analyzed data, and wrote the paper.

ACKNOWLEDGMENTS

We thank the animal care staff of the NIH Clinical Research Facility animal facility. We also thank the staff of the National Cancer Institute, Experimental Transplantation and Immunology Branch flow cytometry core facility. We thank Jeremy Rose and Shayla Duncan for processing patient blood samples. This work was supported by intramural funding of the Center for Cancer Research, National Cancer Institute, NIH and Kite Pharma through a cooperative research and development agreement (CRADA) with the National Cancer Institute (James N. Kochenderfer, principal investigator)

REFERENCES

1. Dotti, G., Gottschalk, S., Savoldo, B., and Brenner, M.K. (2014). Design and development of therapies using chimeric antigen receptor-expressing T cells. Immunol. Rev. *257*, 107–126.
2. Jensen, M.C., and Riddell, S.R. (2015). Designing chimeric antigen receptors to effectively and safely target tumors. Curr. Opin. Immunol. *33*, 9–15.
3. Kochenderfer, J.N., and Rosenberg, S.A. (2013). Treating B-cell cancer with T cells expressing anti-CD19 chimeric antigen receptors. Nat. Rev. Clin. Oncol. *10*, 267–276.
4. Sadelain, M. (2015). CAR therapy: the CD19 paradigm. J. Clin. Invest. *125*, 3392–3400.
5. Eshhar, Z., Waks, T., Gross, G., and Schindler, D.G. (1993). Specific activation and targeting of cytotoxic lymphocytes through chimeric single chains consisting of antibody-binding domains and the gamma or zeta subunits of the immunoglobulin and T-cell receptors. Proc. Natl. Acad. Sci. U S A *90*, 720–724.
6. Geldres, C., Savoldo, B., and Dotti, G. (2016). Chimeric antigen receptor-redirected T cells return to the bench. Semin. Immunol. *28*, 3–9.
7. Porter, D.L., Levine, B.L., Kalos, M., Bagg, A., and June, C.H. (2011). Chimeric antigen receptor-modified T cells in chronic lymphoid leukemia. N. Engl. J. Med. *365*, 725–733.
8. Kochenderfer, J.N., Wilson, W.H., Janik, J.E., Dudley, M.E., Stetler-Stevenson, M., Feldman, S.A., Maric, I., Raffeld, M., Nathan, D.A., Lanier, B.J., et al. (2010). Eradication of B-lineage cells and regression of lymphoma in a patient treated with autologous T cells genetically engineered to recognize CD19. Blood *116*, 4099–4102.
9. Kochenderfer, J.N., Dudley, M.E., Feldman, S.A., Wilson, W.H., Spaner, D.E., Maric, I., Stetler-Stevenson, M., Phan, G.Q., Hughes, M.S., Sherry, R.M., et al. (2012). B-cell depletion and remissions of malignancy along with cytokine-associated toxicity in a clinical trial of anti-CD19 chimeric-antigen-receptor-transduced T cells. Blood *119*, 2709–2720.
10. Kochenderfer, J.N., Dudley, M.E., Kassim, S.H., Somerville, R.P.T., Carpenter, R.O., Stetler-Stevenson, M., Yang, J.C., Phan, G.Q., Hughes, M.S., Sherry, R.M., et al. (2015). Chemotherapy-refractory diffuse large B-cell lymphoma and indolent B-cell malignancies can be effectively treated with autologous T cells expressing an anti-CD19 chimeric antigen receptor. J. Clin. Oncol. *33*, 540–549.
11. Turtle, C.J., Hanafi, L.A., Berger, C., Gooley, T.A., Cherian, S., Hudecek, M., Sommermeyer, D., Melville, K., Pender, B., Budiarto, T.M., et al. (2016). CD19 CAR-T cells of defined CD4+:CD8+ composition in adult B cell ALL patients. J. Clin. Invest. *126*, 2123–2138.
12. Brentjens, R.J., Davila, M.L., Riviere, I., Park, J., Wang, X., Cowell, L.G., Bartido, S., Stefanski, J., Taylor, C., Olszewska, M., et al. (2013). CD19-targeted T cells rapidly induce molecular remissions in adults with chemotherapy-refractory acute lymphoblastic leukemia. Sci. Transl. Med. *5*, 177ra38.
13. Savoldo, B., Ramos, C.A., Liu, E., Mims, M.P., Keating, M.J., Carrum, G., Kamble, R.T., Bollard, C.M., Gee, A.P., Mei, Z., et al. (2011). CD28 costimulation improves expansion and persistence of chimeric antigen receptor-modified T cells in lymphoma patients. J. Clin. Invest. *121*, 1822–1826.
14. Lee, D.W., Kochenderfer, J.N., Stetler-Stevenson, M., Cui, Y.K., Delbrook, C., Feldman, S.A., Fry, T.J., Orentas, R., Sabatino, M., Shah, N.N., et al. (2015). T cells expressing CD19 chimeric antigen receptors for acute lymphoblastic leukaemia in children and young adults: a phase 1 dose-escalation trial. Lancet *385*, 517–528.
15. Maude, S.L., Frey, N., Shaw, P.A., Aplenc, R., Barrett, D.M., Bunin, N.J., Chew, A., Gonzalez, V.E., Zheng, Z., Lacey, S.F., et al. (2014). Chimeric antigen receptor T cells for sustained remissions in leukemia. N. Engl. J. Med. *371*, 1507–1517.
16. Davila, M.L., Riviere, I., Wang, X., Bartido, S., Park, J., Curran, K., Chung, S.S., Stefanski, J., Borquez-Ojeda, O., Olszewska, M., et al. (2014). Efficacy and toxicity management of 19-28z CAR T cell therapy in B cell acute lymphoblastic leukemia. Sci. Transl. Med. *6*, 224ra25.
17. Turtle, C.J., Hanafi, L.A., Berger, C., Hudecek, M., Pender, B., Robinson, E., Hawkins, R., Chaney, C., Cherian, S., Chen, X., et al. (2016). Immunotherapy of non-Hodgkin's lymphoma with a defined ratio of CD8+ and CD4+ CD19-specific chimeric antigen receptor-modified T cells. Sci. Transl. Med. *8*, 355ra116.
18. Kebriaei, P., Singh, H., Huls, M.H., Figliola, M.J., Bassett, R., Olivares, S., Jena, B., Dawson, M.J., Kumaresan, P.R., Su, S., et al. (2016). Phase I trials using Sleeping Beauty to generate CD19-specific CAR T cells. J. Clin. Invest. *126*, 3363–3376.
19. Brudno, J.N., Somerville, R.P.T., Shi, V., Rose, J.J., Halverson, D.C., Fowler, D.H., Gea-Banacloche, J.C., Pavletic, S.Z., Hickstein, D.D., Lu, T.L., et al. (2016). Allogeneic T cells that express an anti-CD19 chimeric antigen receptor induce remissions of B-cell malignancies that progress after allogeneic hematopoietic stem-cell transplantation without causing graft-versus-host disease. J. Clin. Oncol. *34*, 1112–1121.
20. Ali, S.A., Shi, V., Maric, I., Wang, M., Stroncek, D.F., Rose, J.J., Brudno, J.N., Stetler-Stevenson, M., Feldman, S.A., Hansen, B.G., et al. (2016). T cells expressing an

anti-B-cell maturation antigen chimeric antigen receptor cause remissions of multiple myeloma. Blood *128*, 1688–1700.

21. Cruz, C.R.Y., Micklethwaite, K.P., Savoldo, B., Ramos, C.A., Lam, S., Ku, S., Diouf, O., Liu, E., Barrett, A.J., Ito, S., et al. (2013). Infusion of donor-derived CD19-redirected virus-specific T cells for B-cell malignancies relapsed after allogeneic stem cell transplant: a phase 1 study. Blood *122*, 2965–2973.
22. Jensen, M.C., Popplewell, L., Cooper, L.J., DiGiusto, D., Kalos, M., Ostberg, J.R., and Forman, S.J. (2010). Antitransgene rejection responses contribute to attenuated persistence of adoptively transferred CD20/CD19-specific chimeric antigen receptor redirected T cells in humans. Biol. Blood Marrow Transplant. *16*, 1245–1256.
23. Lamers, C.H.J., Willemsen, R., van Elzakker, P., van Steenbergen-Langeveld, S., Broertjes, M., Oosterwijk-Wakka, J., Oosterwijk, E., Sleijfer, S., Debets, R., and Gratama, J.W. (2011). Immune responses to transgene and retroviral vector in patients treated with ex vivo-engineered T cells. Blood *117*, 72–82.
24. Sommermeyer, D., Hill, T., Shamah, S.M., Salter, A.I., Chen, Y., Mohler, K.M., and Riddell, S.R. (2017). Fully human CD19-specific chimeric antigen receptors for T-cell therapy. Leukemia, Published online March 21, 2017. http://dx.doi.org/10.1038/leu.2017.57.
25. Maher, J., Brentjens, R.J., Gunset, G., Rivière, I., and Sadelain, M. (2002). Human T-lymphocyte cytotoxicity and proliferation directed by a single chimeric TCRzeta /CD28 receptor. Nat. Biotechnol. *20*, 70–75.
26. Sadelain, M., Brentjens, R., and Rivière, I. (2013). The basic principles of chimeric antigen receptor design. Cancer Discov. *3*, 388–398.
27. Guest, R.D., Hawkins, R.E., Kirillova, N., Cheadle, E.J., Arnold, J., O'Neill, A., Irlam, J., Chester, K.A., Kemshead, J.T., Shaw, D.M., et al. (2005). The role of extracellular spacer regions in the optimal design of chimeric immune receptors: evaluation of four different scFvs and antigens. J. Immunother. *28*, 203–211.
28. Gargett, T., Yu, W., Dotti, G., Yvon, E.S., Christo, S.N., Hayball, J.D., Lewis, I.D., Brenner, M.K., and Brown, M.P. (2016). GD2-specific CAR T cells undergo potent activation and deletion following antigen encounter but can be protected from activation-induced cell death by PD-1 blockade. Mol. Ther. *24*, 1135–1149.
29. Hudecek, M., Sommermeyer, D., Kosasih, P.L., Silva-Benedict, A., Liu, L., Rader, C., Jensen, M.C., and Riddell, S.R. (2015). The nonsignaling extracellular spacer domain of chimeric antigen receptors is decisive for in vivo antitumor activity. Cancer Immunol. Res. *3*, 125–135.
30. Künkele, A., Johnson, A.J., Rolczynski, L.S., Chang, C.A., Hoglund, V., Kelly-Spratt, K.S., and Jensen, M.C. (2015). Functional tuning of CARs reveals signaling threshold above which CD8+ CTL antitumor potency is attenuated due to cell Fas-FasL-dependent AICD. Cancer Immunol. Res. *3*, 368–379.
31. Brenner, D., Krammer, P.H., and Arnold, R. (2008). Concepts of activated T cell death. Crit. Rev. Oncol. Hematol. *66*, 52–64.
32. Green, D.R., Droin, N., and Pinkoski, M. (2003). Activation-induced cell death in T cells. Immunol. Rev. *193*, 70–81.
33. Brudno, J.N., and Kochenderfer, J.N. (2016). Toxicities of chimeric antigen receptor T cells: recognition and management. Blood *127*, 3321–3330.
34. Long, A.H., Haso, W.M., Shern, J.F., Wanhainen, K.M., Murgai, M., Ingaramo, M., Smith, J.P., Walker, A.J., Kohler, M.E., Venkateshwara, V.R., et al. (2015). 4-1BB costimulation ameliorates T cell exhaustion induced by tonic signaling of chimeric antigen receptors. Nat. Med. *21*, 581–590.
35. Sallusto, F., Lenig, D., Förster, R., Lipp, M., and Lanzavecchia, A. (1999). Two subsets of memory T lymphocytes with distinct homing potentials and effector functions. Nature *401*, 708–712.
36. Wherry, E.J., and Kurachi, M. (2015). Molecular and cellular insights into T cell exhaustion. Nat. Rev. Immunol. *15*, 486–499.
37. Combadière, B., Freedman, M., Chen, L., Shores, E.W., Love, P., and Lenardo, M.J. (1996). Qualitative and quantitative contributions of the T cell receptor zeta chain to mature T cell apoptosis. J. Exp. Med. *183*, 2109–2117.
38. Kochenderfer, J.N., Yu, Z., Frasheri, D., Restifo, N.P., and Rosenberg, S.A. (2010). Adoptive transfer of syngeneic T cells transduced with a chimeric antigen receptor that recognizes murine CD19 can eradicate lymphoma and normal B cells. Blood *116*, 3875–3886.
39. Zhao, Y., Wang, Q.J., Yang, S., Kochenderfer, J.N., Zheng, Z., Zhong, X., Sadelain, M., Eshhar, Z., Rosenberg, S.A., and Morgan, R.A. (2009). A herceptin-based chimeric antigen receptor with modified signaling domains leads to enhanced survival of transduced T lymphocytes and antitumor activity. J. Immunol. *183*, 5563–5574.
40. Evans, E.J., Esnouf, R.M., Manso-Sancho, R., Gilbert, R.J.C., James, J.R., Yu, C., Fennelly, J.A., Vowles, C., Hanke, T., Walse, B., et al. (2005). Crystal structure of a soluble CD28-Fab complex. Nat. Immunol. *6*, 271–279.
41. Leahy, D.J., Axel, R., and Hendrickson, W.A. (1992). Crystal structure of a soluble form of the human T cell coreceptor CD8 at 2.6 A resolution. Cell *68*, 1145–1162.
42. Pageon, S.V., Tabarin, T., Yamamoto, Y., Ma, Y., Bridgeman, J.S., Cohnen, A., Benzing, C., Gao, Y., Crowther, M.D., Tungatt, K., et al. (2016). Functional role of T-cell receptor nanoclusters in signal initiation and antigen discrimination. Proc. Natl. Acad. Sci. U S A *113*, E5454–E5463.
43. van der Merwe, P.A., and Dushek, O. (2011). Mechanisms for T cell receptor triggering. Nat. Rev. Immunol. *11*, 47–55.
44. Whitlow, M., Bell, B.A., Feng, S.L., Filpula, D., Hardman, K.D., Hubert, S.L., Rollence, M.L., Wood, J.F., Schott, M.E., Milenic, D.E., et al. (1993). An improved linker for single-chain Fv with reduced aggregation and enhanced proteolytic stability. Protein Eng. *6*, 989–995.
45. Kochenderfer, J.N., Dudley, M.E., Carpenter, R.O., Kassim, S.H., Rose, J.J., Telford, W.G., Hakim, F.T., Halverson, D.C., Fowler, D.H., Hardy, N.M., et al. (2013). Donor-derived CD19-targeted T cells cause regression of malignancy persisting after allogeneic hematopoietic stem cell transplantation. Blood *122*, 4129–4139.
46. Wherry, E.J. (2011). T cell exhaustion. Nat. Immunol. *12*, 492–499.
47. Klebanoff, C.A., Gattinoni, L., Palmer, D.C., Muranski, P., Ji, Y., Hinrichs, C.S., Borman, Z.A., Kerkar, S.P., Scott, C.D., Finkelstein, S.E., et al. (2011). Determinants of successful CD8+ T-cell adoptive immunotherapy for large established tumors in mice. Clin. Cancer Res. *17*, 5343–5352.
48. Chinnasamy, D., Yu, Z., Theoret, M.R., Zhao, Y., Shrimali, R.K., Morgan, R.A., Feldman, S.A., Restifo, N.P., and Rosenberg, S.A. (2010). Gene therapy using genetically modified lymphocytes targeting VEGFR-2 inhibits the growth of vascularized syngenic tumors in mice. J. Clin. Invest. *120*, 3953–3968.
49. Kochendefer, J.N., Somerville, R., Lu, T., Shi, V., Bot, A., Rossi, J., Xue, A., Goff, S.L., Yang, J.C., Sherry, R.M., et al. (2017). Lymphoma remissions caused by anti-CD19 chimeric antigen receptor t cells are associated with high serum inerleukin-15 levels. J. Clin. Oncol. *35*, 1803–1813.
50. Eisenman, J., Ahdieh, M., Beers, C., Brasel, K., Kennedy, M.K., Le, T., Bonnert, T.P., Paxton, R.J., and Park, L.S. (2002). Interleukin-15 interactions with interleukin-15 receptor complexes: characterization and species specificity. Cytokine *20*, 121–129.
51. Carpenter, R.O., Evbuomwan, M.O., Pittaluga, S., Rose, J.J., Raffeld, M., Yang, S., Gress, R.E., Hakim, F.T., and Kochenderfer, J.N. (2013). B-cell maturation antigen is a promising target for adoptive T-cell therapy of multiple myeloma. Clin. Cancer Res. *19*, 2048–2060.
52. King, D.J., Rao-Naik, C., Pan, C., Cardarelli, J., and Blanset, D. April 2010. Human antibodies that bind CD19 and uses thereof. U.S. patent US2010/0104509 A1.
53. Yang, S., Dudley, M.E., Rosenberg, S.A., and Morgan, R.A. (2010). A simplified method for the clinical-scale generation of central memory-like CD8+ T cells after transduction with lentiviral vectors encoding antitumor antigen T-cell receptors. J. Immunother. *33*, 648–658.
54. Kochenderfer, J.N., Feldman, S.A., Zhao, Y., Xu, H., Black, M.A., Morgan, R.A., Wilson, W.H., and Rosenberg, S.A. (2009). Construction and preclinical evaluation of an anti-CD19 chimeric antigen receptor. J. Immunother. *32*, 689–702.
55. Hermans, I.F., Silk, J.D., Yang, J., Palmowski, M.J., Gileadi, U., McCarthy, C., Salio, M., Ronchese, F., and Cerundolo, V. (2004). The VITAL assay: a versatile fluorometric technique for assessing CTL- and NKT-mediated cytotoxicity against multiple targets in vitro and in vivo. J. Immunol. Methods *285*, 25–40.
56. Berman, H.M., Westbrook, J., Feng, Z., Gilliland, G., Bhat, T.N., Weissig, H., Shindyalov, I.N., and Bourne, P.E. (2000). The Protein Data Bank. Nucleic Acids Res. *28*, 235–242.

YMTHE, Volume *25*

Supplemental Information

Function of Novel Anti-CD19 Chimeric Antigen Receptors with Human Variable Regions Is Affected by Hinge and Transmembrane Domains

Leah Alabanza, Melissa Pegues, Claudia Geldres, Victoria Shi, Jed J.W. Wiltzius, Stuart A. Sievers, Shicheng Yang, and James N. Kochenderfer

Supplemental Figure 1

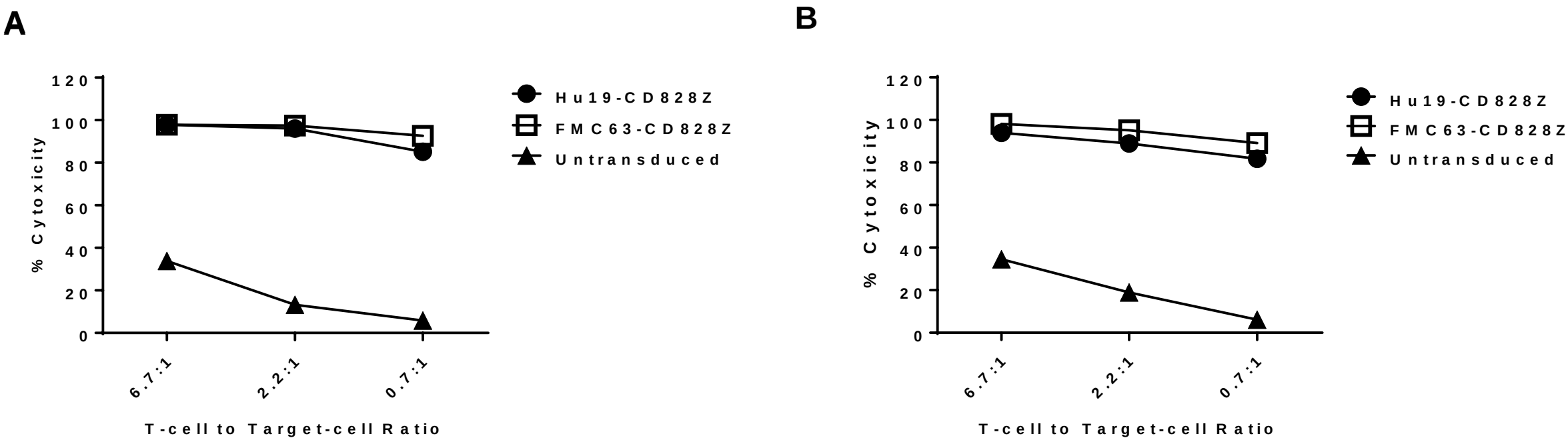

T cells from the same patient were transduced with either Hu19-CD828Z or FMC63-CD828Z. These T cells were tested in 4 hour cytotoxity assays. T cells were cultured at the indicated T cell to target cell ratios with either NALM6 (A) or Toledo (B) target cells. The mean and standard error of the mean cytotoxicity are shown. No substantial difference in cytotoxicity between the 2 CARs was detected.

Supplemental Figure 2: in vivo comparison of FMC63-CD828Z and Hu19-CD828Z

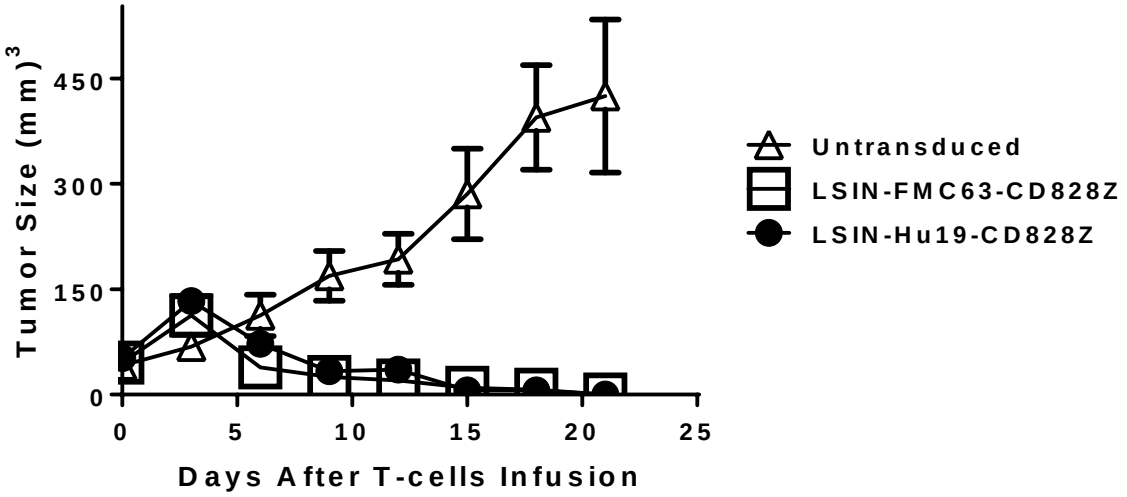

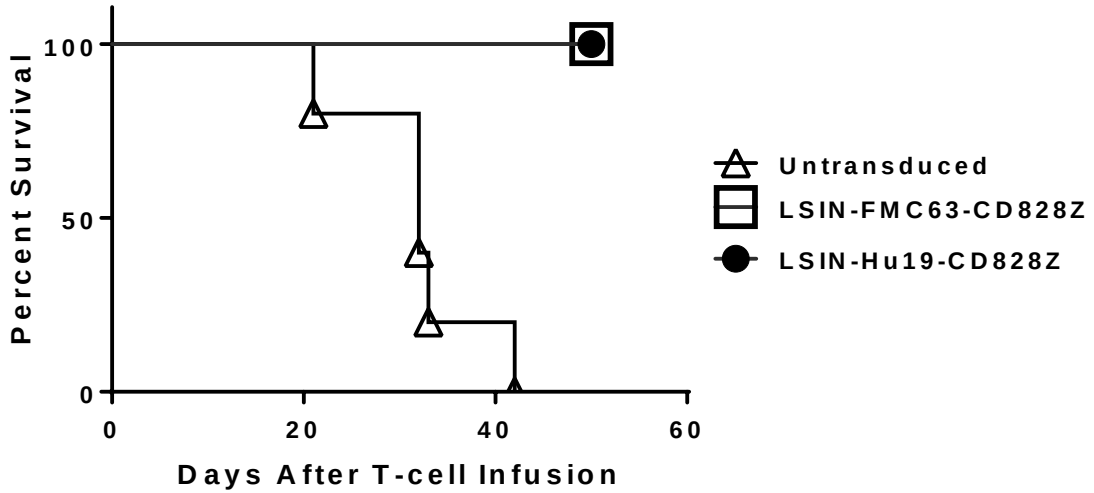

NALM6 tumors were established in immunocompromised NSG mice. The mice then received infusions of 8 million T cells transduced with LSIN-FMC63-CD828Z or LSIN-Hu19-CD828Z or Untransduced T cells. Tumors were measured every 3 days in a blinded manner. There were 5 mice in each group. The tumor sizes and the survival of the mice are shown.

Supplemental Table 1: Raw IFN-gamma ELISA data from Figure 2

	Nalm-6	NGFR-K562	CAR %
Patient 1 Hu19-28z	12368	111	65
Patient 1 Hu19-828z	3285	151	77
Patient 2 Hu19-28z	11589	44	55
Patient 2 Hu19-828z	3617	123	74
Patient 3 Hu19-28z	7047	29	57
Patient 3 Hu19-828z	2665	68	64
Patient 4 Hu19-28z	3637	25	66
Patient 4 Hu19-828z	1728	36	75
Patient 5 Hu19-28z	12770	189	39
Patient 5 Hu19-828z	5469	203	45

Cultured T cells from the indicated patients were transduced with the indicated CARs and cultured overnight with the indicated target cells. After the overnight incubation, a standard ELISA assay was performed on the culture supernatant. NALM6 is $CD19^{+}$ and NGFR-K562 is CD19-negative. The percentage of the T cells expressing the indicated CAR is given as the CAR %. All values are in pg/mL. The normalized version of these results is in Figure 2G.

Supplemental Table 2: Raw TNFα ELISA data from Figure 2

	Nalm-6	NGFR-K562	CAR %
Patient 1 Hu19-28z	1558	<40	65
Patient 1 Hu19-828z	530	<40	77
Patient 2 Hu19-28z	1663	<40	55
Patient 2 Hu19-828z	894	<40	74
Patient 3 Hu19-28z	2224	0	57
Patient 3 Hu19-828z	840	0	64
Patient 4 Hu19-28z	1797	25	66
Patient 4 Hu19-828z	771	19	75
Patient 5 Hu19-28z	1988	35	39
Patient 5 Hu19-828z	950	35	45

Cultured T cells from the indicated patients were transduced with the indicated CARs and cultured overnight with the indicated target cells. After the overnight incubation, a standard ELISA assay was performed on the culture supernatant. NALM6 is $CD19^{+}$ and NGFR-K562 is CD19-negative. All values are in pg/mL. The percentage of the T cells expressing the indicated CAR is given as the CAR %. The normalized version of these results is in Figure 2H.

Supplemental Table 3: Raw IFN-gamma ELISA data from Figure 3

IFN-gamma			
	CD19-K562	NGFR-K562	CAR %
Patient 1 FMC63-28z	81568	202	75
Patient 1 FMC63-828z	29983	133	89
Patient 2 FMC63-28z	69146	170	79
Patient 2 FMC63-828z	21771	144	93
Patient 3 FMC63-28z	74756	462	73
Patient 3 FMC63-828z	36054	155	73
Patient 4 FMC63-28z	57845	985	84
Patient 4 FMC63-828z	19888	254	93
Patient 5 FMC63-28z	20694	282	71
Patient 5 FMC63-828z	8795	72	87

Cultured T cells from the indicated patients were transduced with the indicated CARs and cultured overnight with the indicated target cells. After the overnight incubation, a standard ELISA assay was performed on the culture supernatant. CD19-K562 is $CD19^{+}$ and NGFR-K562 is CD19-negative. All values are in pg/mL. The percentage of the T cells expressing the indicated CAR is given as the CAR %. The normalized version of these results is in Figure 3E.

Supplemental Table 4: Raw TNF-α ELISA data from Figure 3

	CD19-K562	NGFR-K562	CAR %
Patient 1 FMC63-28z	9671	60	75
Patient 1 FMC63-828z	5510	36	89
Patient 2 FMC63-28z	2732	21	79
Patient 2 FMC63-828z	1552	16	93
Patient 3 FMC63-28z	6243	89	73
Patient 3 FMC63-828z	2354	32	73
Patient 4 FMC63-28z	9865	100	84
Patient 4 FMC63-828z	3238	<40	93
Patient 5 FMC63-28z	15518	671	71
Patient 5 FMC63-828z	7462	53	87

Cultured T cells from the indicated patients were transduced with the indicated CARs and cultured overnight with the indicated target cells. After the overnight incubation, a standard ELISA assay was performed on the culture supernatant. CD19-K562 is $CD19^+$ and NGFR-K562 is CD19-negative. All values are in pg/mL. The percentage of the T cells expressing the indicated CAR is given as the CAR %. The normalized version of these results is in Figure 3F.

Supplemental Table 5: Raw IL-2 ELISA data from Figure 4

	Nalm-6	NGFR-K562	CAR %
Patient 1 Hu19-28z	373	12	62
Patient 1 Hu19-828z	15	12	74
Patient 2 Hu19-28z	1226	17	34
Patient 2 Hu19-828z	268	20	46
Patient 3 Hu19-28z	197	20	68
Patient 3 Hu19-828z	44	22	80
Patient 4 Hu19-28z	886	126	60
Patient 4 Hu19-828z	714	147	75
Patient 5 Hu19-28z	1024	68	46
Patient 5 Hu19-828z	302	40	50
Patient 6 Hu19-28z	1404	16	57
Patient 6 Hu19-828z	81	16	64

Cultured T cells from the indicated patients were transduced with the indicated CARs and cultured overnight with the indicated target cells. After the overnight incubation, a standard ELISA assay was performed on the culture supernatant. NALM6 is $CD19^{+}$ and NGFR-K562 is CD19-negative. All values are in pg/mL. The percentage of the T cells expressing the indicated CAR is given as the CAR %. The normalized version of these results is in Figure 4E.

Supplemental Table 6: absolute values of median fluorescent intensity of phosphorylated tyrosine-142 in CD3ζ ITAMs of CAR T cells

Patient	Hu19-CD828Z plus NALM6	Hu19-CD828Z plus NGFR-K562	Hu19-28Z plus NALM6	Hu19-28Z plus NGFR-K562
1	270	245	211	140
2	294	211	235	158
3	348	299	267	190
4	376	347	268	186

All numbers are median fluorescent intensity.

T cells expressing the indicated CARs were cultured with the indicated target cells.

Supplemental Figure 3: Comparison of AICD with Hu19 versus FMC63 scFvs

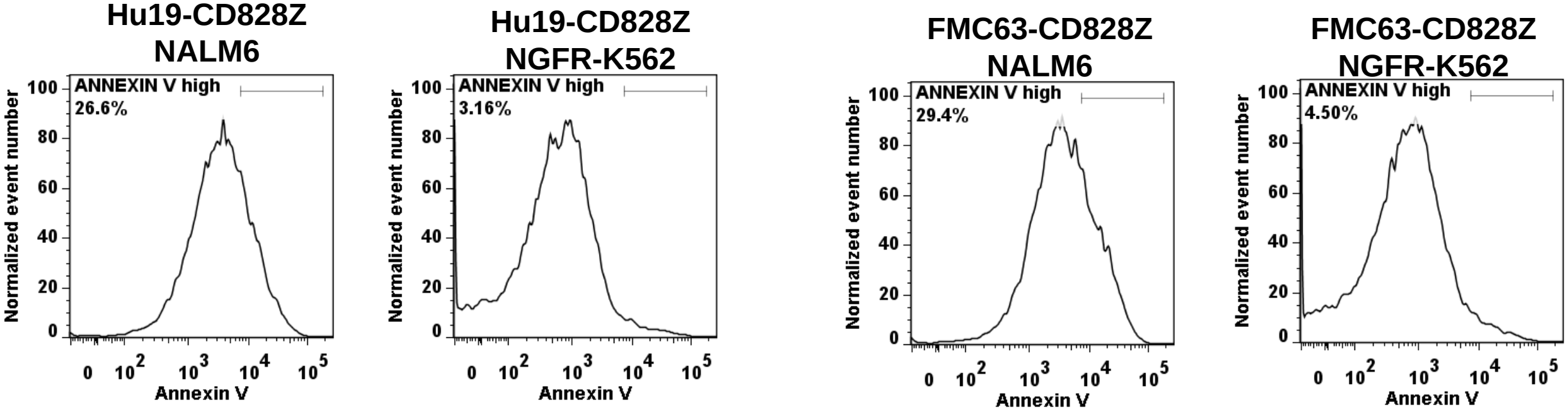

Levels of activation-induced cell death (AICD) were similar in T cells expressing either Hu19-CD828Z or FMC63-CD828Z. T cells from the same donor that were transduced with either Hu19-CD828Z or FMC63-CD828Z were cultured with either $CD19^{+}$ NALM6 cells or CD19-negative NGFR-K562 cells. In the figure, the CAR that T cells were transduced with is on the top line of the label and the target cell is on the bottom line of the label. This is a representative example of 2 different experiments with cells from different donors.

Supplemental Figure 4: memory markers at day 7 after culture initiation

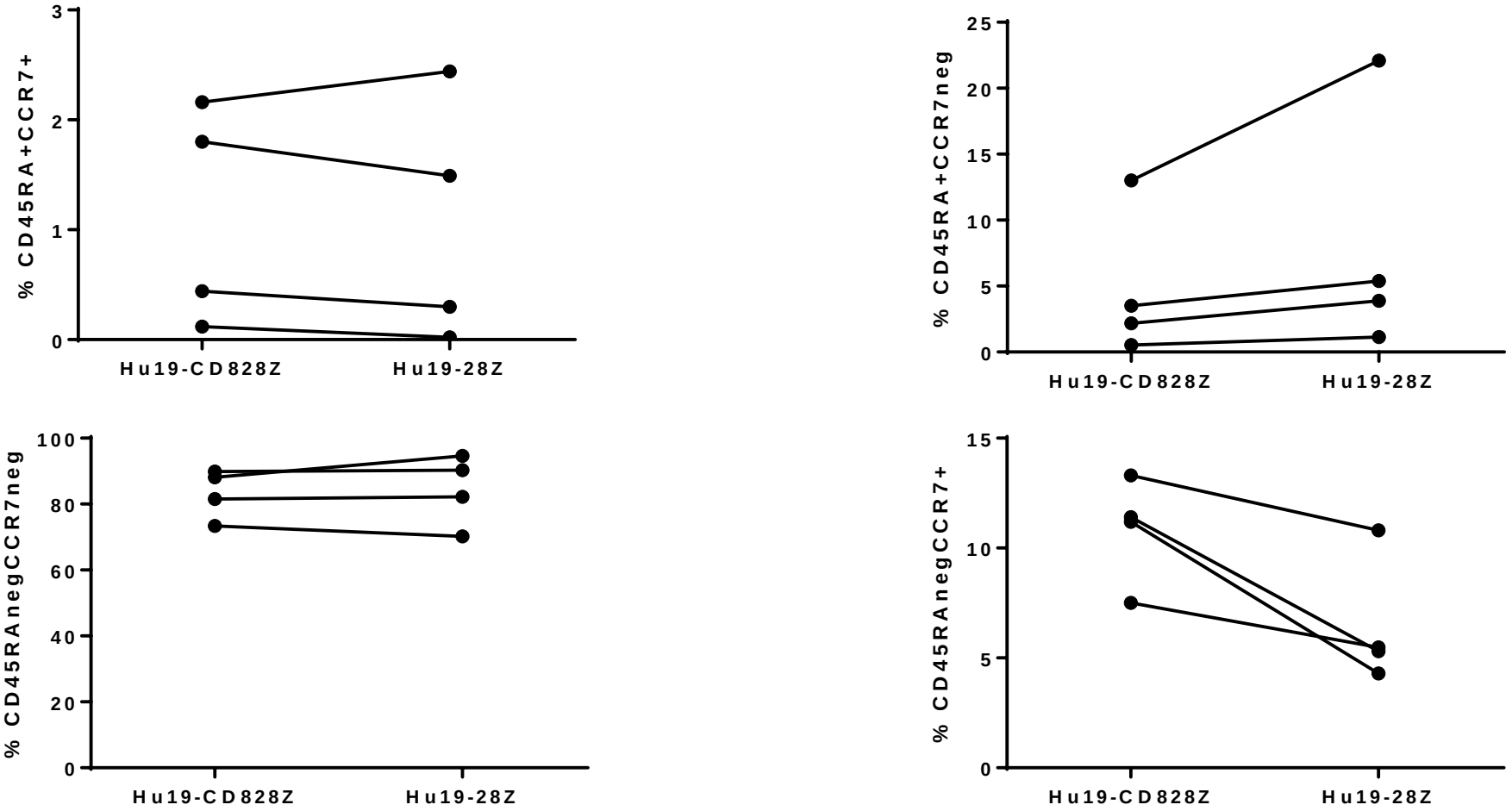

PBMC from 4 patients were activated with an anti-CD3 antibody and transduced with either Hu19-CD828Z or Hu19-28Z. On day 7 after culture initiation, the cells were stained for the indicated markers. Plots of CCR7 versus CD45RA gated on live, $CD3^+$, CAR^+ lymphocytes were analyzed. There was a statistically-significant difference between Hu19-CD828Z and Hu19-28Z only for the %CD45RA-negative, $CCR7^+$ central memory T cells (P=0.039, paired two-tailed t test).

Supplemental Figure 5A: Activation and exhaustion markers at day 7 after culture initiation

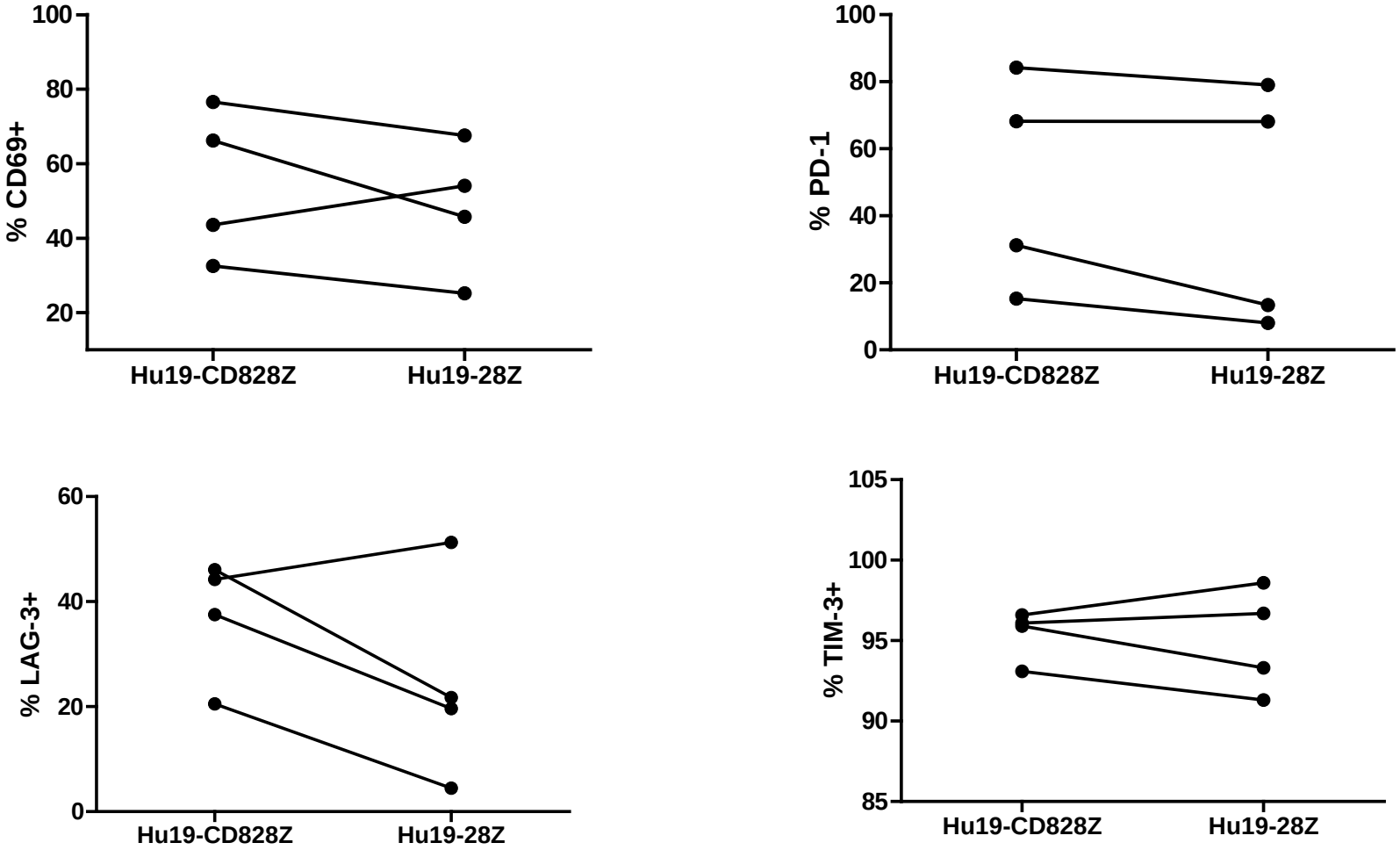

PBMC from 4 patients were activated with an anti-CD3 antibody and transduced with either Hu19-CD828Z or Hu19-28Z. On day 7 after culture initiation, the cells were stained for the indicated markers. Plots are gated on live, $CD3^+$, CAR^+ lymphocytes. There was not a statistically-significant difference between Hu19-CD828Z and Hu19-28Z for CD69, PD-1, LAG-3, or TIM-3.

Supplemental Figure 5B: Activation and exhaustion markers at day 7 after culture initiation

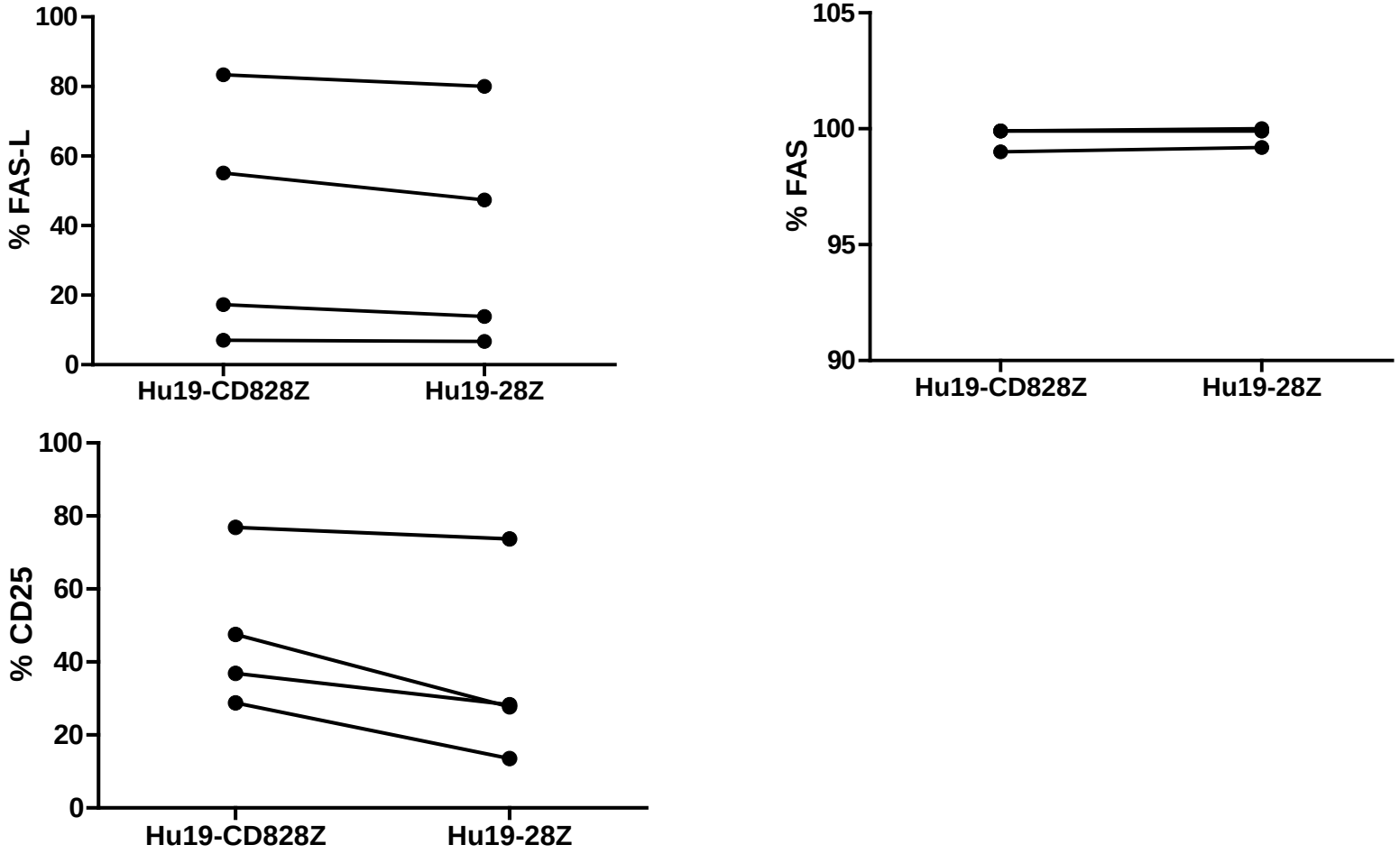

PBMC from 4 patients were activated with an anti-CD3 antibody and transduced with either Hu19-CD828Z or Hu19-28Z. On day 7 after culture initiation, the cells were stained for the indicated markers. Plots are gated on live, $CD3^+$, CAR^+ lymphocytes. There was not a statistically-significant difference between Hu19-CD828Z and Hu19-28Z for FAS-L or FAS expression. CD25 expression was slightly lower on Hu19-28Z T cells (P=0.049, paired 2-tailed t test).

Supplemental Figure 6

Fas ligand

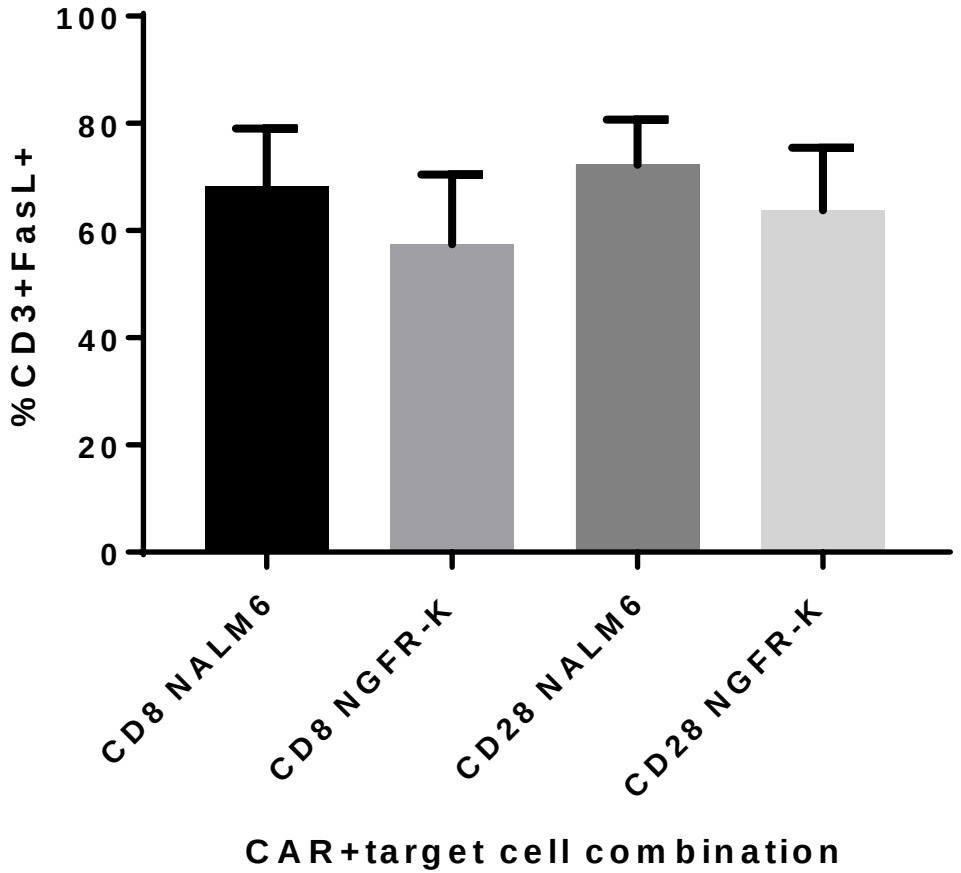

T cells from 4 patients were transduced with either Hu19-CD828Z (CD8 on x-axis label) or Hu19-28Z (28 on x-axis label). The T cells were stimulated with irradiated CD19-K562 cells on day 7 and day 10 after initiation of the cultures. On day 12 after culture initiation, the T cells were cultured overnight with either $CD19^+$ NALM6 cells (NALM6 on x-axis label) or CD19-negative NGFR-K562 cells (NGFR-K on x-axis label). FasL (Fas ligand) staining was conducted. The mean (+ standard error of mean) percentage of $CD3^+$ CAR^+ cells that expressed FasL is shown. There was not a statistically significant difference between the different groups.

Supplemental Figure 7

T cells expressing FMC63-28Z underwent activation-induced cell death in vitro

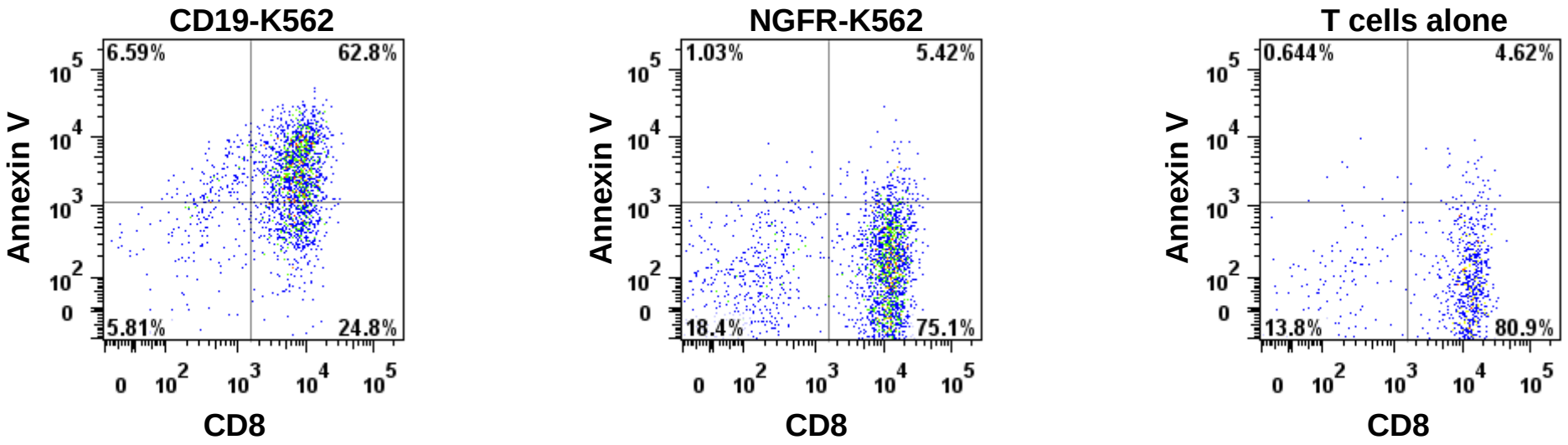

T cells expressing FMC63-28Z were cultured overnight with $CD19^+$ CD19-K562 cells or CD19-negative NGFR-K562 cells. CAR T cells were also cultured alone. At the end of the culture period, cells were stained with annexin V to detect apoptotic cells. Plots are gated on live $CD3^+$, CAR^+ cells. CAR T cells were detected by anti-Fab staining. The percentage of CAR^+ cells undergoing apoptosis increased in a CD19-specific manner.

Supplemental Figure 8

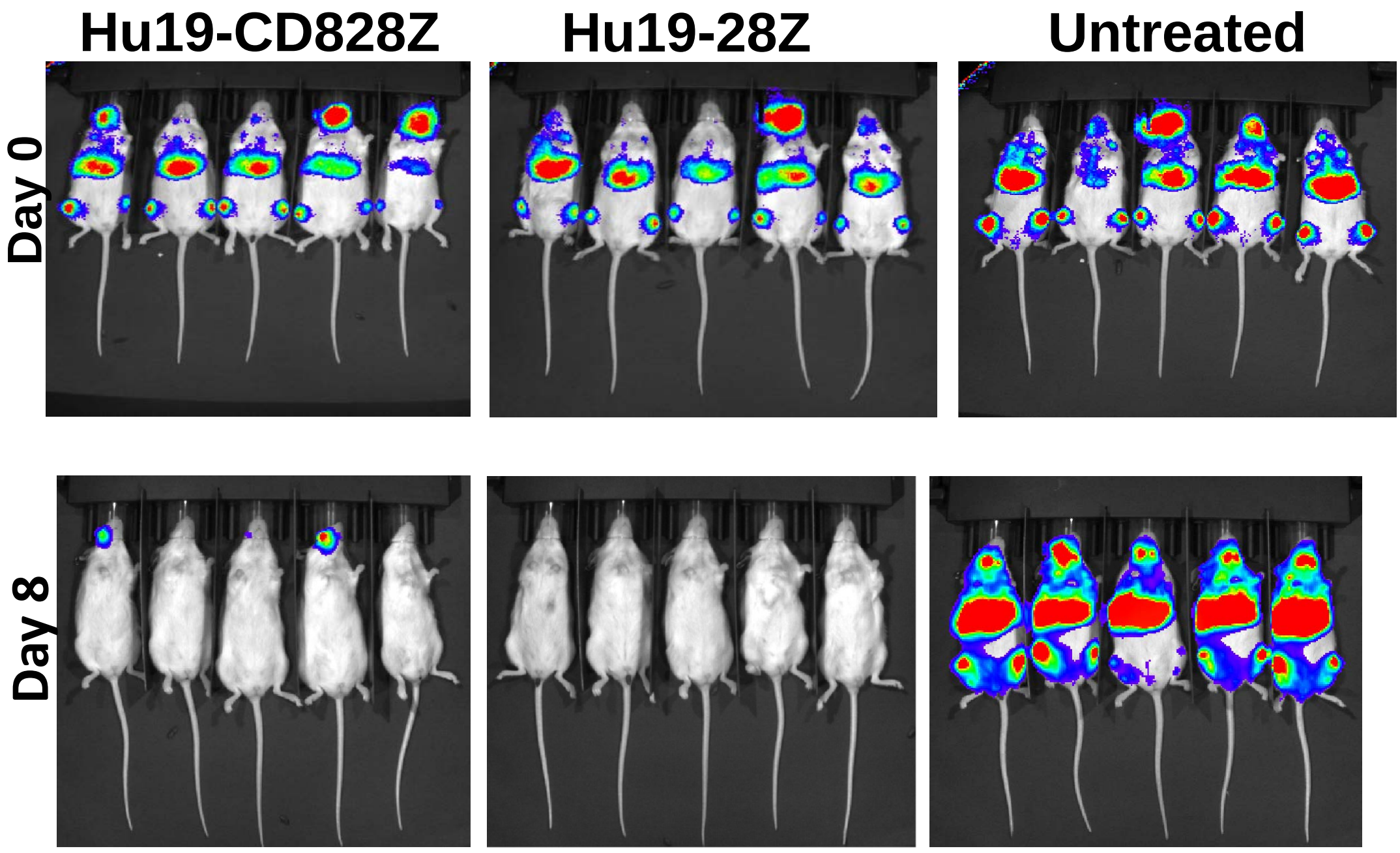

Bioluminescent images of mice bearing NALM6-GL. The groups were either left untreated or infused with $4x10^6$ T cells expressing either Hu19-CD828Z or Hu19-28Z. Images shown were captured on days 0, 8, 16, and 24 after CAR T-cell infusion. One of 2 experiments with very similar results is shown. Units are in photons/second/square centimeter/steradian $x10^8$ at days 8, 16 and 24 and $x10^6$ at day 0. Red is the color of most intense bioluminescence, and blue is the color of least intense bioluminescence.

Supplemental Figure 9

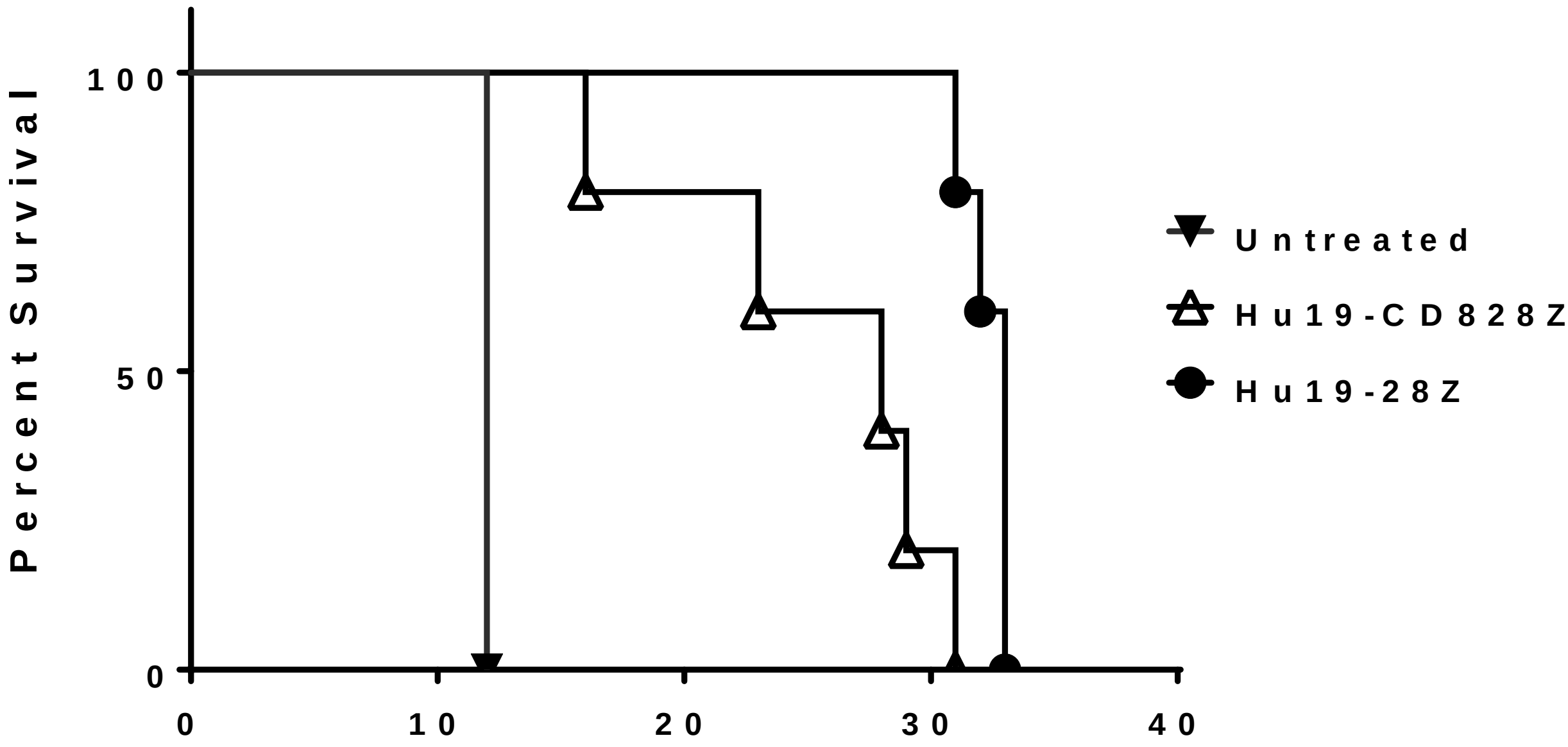

Survival of NALM6-GL bearing mice after treatment with Hu19-28Z or Hu19-CD828Z or no treatment (n = 5 mice for all groups). *P* = 0.0027 for the comparison of Hu19-28Z vs. untreated; *P* = 0.0027 for the comparison of Hu19-CD828Z vs. untreated; *P* = 0.0044 for the comparison of Hu19-CD828Z vs. Hu19-28Z. Comparisons made by the log-rank test. Very similar results were obtained in 2 separate experiments with T cells from different donors.